RESEARCH PAPER
https://doi.org/10.1071/SB23011

Australian Systematic Botany

Plastid phylogenomics of the *Eriostemon* group (Rutaceae; Zanthoxyloideae): support for major clades and investigation of a backbone polytomy

Harvey K. Orel[A,*], Todd G. B. McLay[A,B], Will C. Neal[A], Paul I. Forster[C] and Michael J. Bayly[A]

For full list of author affiliations and declarations see end of paper

***Correspondence to:**
Harvey K. Orel
School of Biosciences, The University of Melbourne, Parkville, Vic. 3010, Australia
Email: horel@student.unimelb.edu.au

Handling Editor:
Jeremy Bruhl

ABSTRACT

Most of Australia's sclerophyllous Rutaceae belong to a clade informally known as the '*Eriostemon* group' (including 16 genera, ~209 species). We investigated generic relationships in this group using analyses of complete plastome sequence data for 60 species and analyses of a supermatrix including sequences of four plastome spacer regions for 22 additional species. Maximum likelihood, Bayesian inference, and shortcut coalescent phylogenetic analyses produced congruent phylogenies that were highly supported, except for a series of short unsupported branches in the backbone of the *Eriostemon* group. We found high support for four major clades branching from this polytomy and discuss evolutionary inferences of generic relationships in each lineage. In an effort to resolve the polytomy, we analysed gene tree topologies in tree space, phylogenetic informativeness with likelihood mapping, and conducted topology tests to assess support for all possible topological resolutions of the polytomy. These approaches did not clarify the polytomy, which may be caused by insufficient data, features of plastome evolution, or rapid radiation. Results from analyses of the combined supermatrix dataset suggest that *Philotheca* section *Philotheca* is paraphyletic with regards to *Drummondita* and *Geleznowia*. In all phylogenies, *Philotheca* sections *Corynonema* and *Cyanochlamys* were not placed with other members of *Philotheca*.

Keywords: *Asterolasia*, Australasia, Australia, *Chorilaena*, *Correa*, *Crowea*, *Diplolaena*, *Drummondita*, *Eriostemon*, *Geleznowia*, *Halfordia*, *Leionema*, likelihood mapping, *Muiriantha*, *Myrtopsis*, *Nematolepis*, *Neoschmidia*, *Phebalium*, *Philotheca*, polytomy, Rutaceae, topology tests, tree space.

Introduction

The Rutaceae is a globally distributed angiosperm family in the order Sapindales that is well-represented in Australia (Orchard 1999). The first major treatments of the family were provided by Engler (1874, 1896, 1931), who placed the Australasian members of the family across four subfamilies (Aurantioideae, Flindersioideae, Rutoideae, and Toddalioideae) and five tribes (Aurantieae, Boronieae, Flindersieae, Toddalieae and Zanthoxyleae). Most Australian taxa were placed in Boronieae, a tribe that Engler (1931) distinguished from the other tribes in subfamily Rutoideae by a broad combination of features pertaining to habit, flower and cotyledon characters, as well as geographic distribution. Subsequent classifications by da Silva *et al.* (1988) and Hartley (1995, 2003) proposed re-adjustments to the limits of the tribe, but maintained Engler's (1931) sentiment that the Boronieae predominantly encompasses a species-rich group of sclerophyllous Australian taxa, that chiefly occur outside of rainforests. From morphological analysis, Armstrong (1991) suggested that the tribe was not monophyletic. Several molecular phylogenies published since these works have confirmed that the tribe is polyphyletic (Groppo *et al.* 2008, 2012; Bayly *et al.* 2013; Appelhans *et al.* 2021; Duretto *et al.* 2023; Joyce *et al.* 2023). These have established that *Boronia* Sm.,

Received: 28 April 2023
Accepted: 1 August 2023
Published: 22 August 2023

Cite this:
Orel HK *et al.* (2023)
Australian Systematic Botany
36(5), 355–385. doi:10.1071/SB23011

Cyanothamnus Lindl., *Neobyrnesia* J.A.Armstr. and *Zieria* Sm. form a clade with members of the *Euodia* J.R.Forst. & G.Forst. alliance (*sensu* Kubitzki *et al.* 2011; e.g. *Acronychia* J.R.Forst & G.Forst., *Brombya* F.Muell., *Medicosma* Hook.f., *Melicope* J.R.Forst & G.Forst., *Perryodendron* T.G.Hartley, *Picrella* Baill., *Tetractomia* Hook.f.) that is sister to a clade containing most of the genera historically placed in Boronieae (*Asterolasia* F.Muell., *Chorilaena* Endl., *Correa* Andrews, *Crowea* Sm., *Diplolaena* R.Br., *Drummondita* Harv., *Eriostemon* Sm., *Geleznowia* Turcz., *Leionema* (F.Muell.) Paul G.Wilson, *Muiriantha* C.A.Gardner, *Nematolepis* Turcz., *Phebalium* Vent., *Philotheca* Rudge). Also included in the latter clade are *Halfordia* F.Muell., *Myrtopsis* Engl. and *Neoschmidia* T.G.Hartley, three genera that recent taxonomists have not considered part of tribe Boronieae (Hartley 2001, 2003; Kubitzki *et al.* 2011). For ease of reference, we hereafter refer to this clade (equivalent to 'Clade C' in the work of Bayly *et al.* 2013) as the *Eriostemon* group.

The *Eriostemon* group includes 16 genera and ~209 species that almost all occur naturally in Australia. The exceptions to this are the New Caledonian genera *Myrtopsis* (~9 spp.) and *Neoschmidia* (2 spp.), and the New Zealand-endemic *Leionema nudum* (Hook.) Paul G.Wilson. The group is most diverse in the south-east and south-west of Australia, with only a few species found in the northern half of the continent. Plants in the group occur in various environments, ranging through rainforests, woodlands, savanna, coastal and montane heathlands, semi-arid scrub and desert shrubland. However, most commonly members of the group occur in sclerophyll woodlands and forests that are typically dominated by eucalypts.

The diverse distribution of the group is matched by a large degree of morphological diversity. Plants range in habit from small shrubs to trees (but are mostly small-leaved shrubs); leaf phyllotaxy varies between opposite and alternate arrangement (mostly alternate); inflorescences may be axillary or terminal; flowers are four- or five-merous and solitary or in clusters, cymes or racemes; and fruits range from fleshy drupes to (most commonly) dry, dehiscent follicles.

Because of this morphological diversity and extensive morphological homoplasy (Armstrong 1991), generic classification of the group has been historically difficult. Some genera (e.g. *Geleznowia*) display a range of highly derived apomorphic characters that support their monophyly but make them hard to place with respect to other genera due to lack of synapomorphies. Others (e.g. *Philotheca*) are indiscrete in their morphological delimitation and lack strongly defined apomorphies to support their monophyly. This combination of taxa with either highly apomorphic or plesiomorphic morphologies has hindered classification of the whole group.

Several studies have investigated aspects of relationships in the *Eriostemon* group by using molecular data. These have provided useful resolution of species-level relationships in some genera (e.g. Othman *et al.* 2010; Bayly *et al.* 2016; French *et al.* 2016; Batty *et al.* 2022), and have established the monophyly of several genera (Mole *et al.* 2004; Duretto *et al.* 2023). Despite this body of work, relationships between genera remain poorly understood; the few molecular studies that have sampled the Rutaceae thoroughly have been limited by relatively low taxon sampling from the *Eriostemon* group or low amounts of sequence data for phylogenetic analysis (e.g. Mole *et al.* 2004; Bayly *et al.* 2013; Appelhans *et al.* 2021; Duretto *et al.* 2023), leading to poor support for many branches above genus level. Consequently, relationships among genera are unclear and several potential taxonomic issues have been identified but left unresolved.

One major taxonomic issue is the current delimitation of *Philotheca*, which has been recovered as polyphyletic in several molecular phylogenies but has not been reclassified (Bayly *et al.* 2013; Appelhans *et al.* 2021). As currently circumscribed, there are four sections in *Philotheca* (Wilson 2013*a*), with 54 accepted, named species and one phrase-named species (Australian Plant Census, see https://biodiversity.org.au/nsl/services/search/taxonomy, accessed April 2023). The type section, *Philotheca* section *Philotheca* (34 spp.; eastern and south-western Australia, Fig. 1*c*), is more closely related to *Drummondita* (11 spp.; Western Australia, Northern Territory and Queensland, Fig. 1*b*) and *Geleznowia* (2 spp.; Western Australia, Fig. 1*a*) than the three other sections of *Philotheca* (Bayly *et al.* 2013; Appelhans *et al.* 2021). *Philotheca* section *Erionema* (F.Muell.) Paul G.Wilson (15 spp.; 14 eastern Australia, one south-western Australia, Fig. 1*d*), is a monophyletic group that is well-defined by a number of synapomorphies (Wilson 1998*a*; Bayly 2001; Batty *et al.* 2022). *Philotheca* section *Corynonema* (Paul G.Wilson) Paul G.Wilson (3 spp.; south-eastern and south-western Australia, Fig. 1*f*) and *Philotheca* section *Cyanochlamys* (F.Muell.) Paul G.Wilson (2 spp.; south-western Australia, Fig. 1*e*) are small sections with diverse floral and vegetative morphologies. The phylogenetic positions of the three non-type sections of *Philotheca* in the *Eriostemon* group are yet to be adequately determined.

Despite evidence for the polyphyly of *Philotheca*, relationships among *Philotheca* section *Philotheca*, *Drummondita* and *Geleznowia* have not yet been resolved well-enough to determine an appropriate taxonomic treatment. In particular, taxonomic changes have not been applied to *Philotheca* because of uncertainty surrounding the monophyly of section *Philotheca*; it is not clear whether *Geleznowia* and *Drummondita* are sisters to section *Philotheca*, or nested within it. In the former case, it could be possible to retain these distinctive and long-recognised taxa as separate genera; in the latter case, there would be grounds for including *Geleznowia* and *Drummondita* in *Philotheca*. Morphologically, *Drummondita*, *Geleznowia* and *Philotheca* section *Philotheca* are mostly distinct in their flowers, which bear differences that are the result of different pollination syndromes (Armstrong 1987). *Drummondita* has

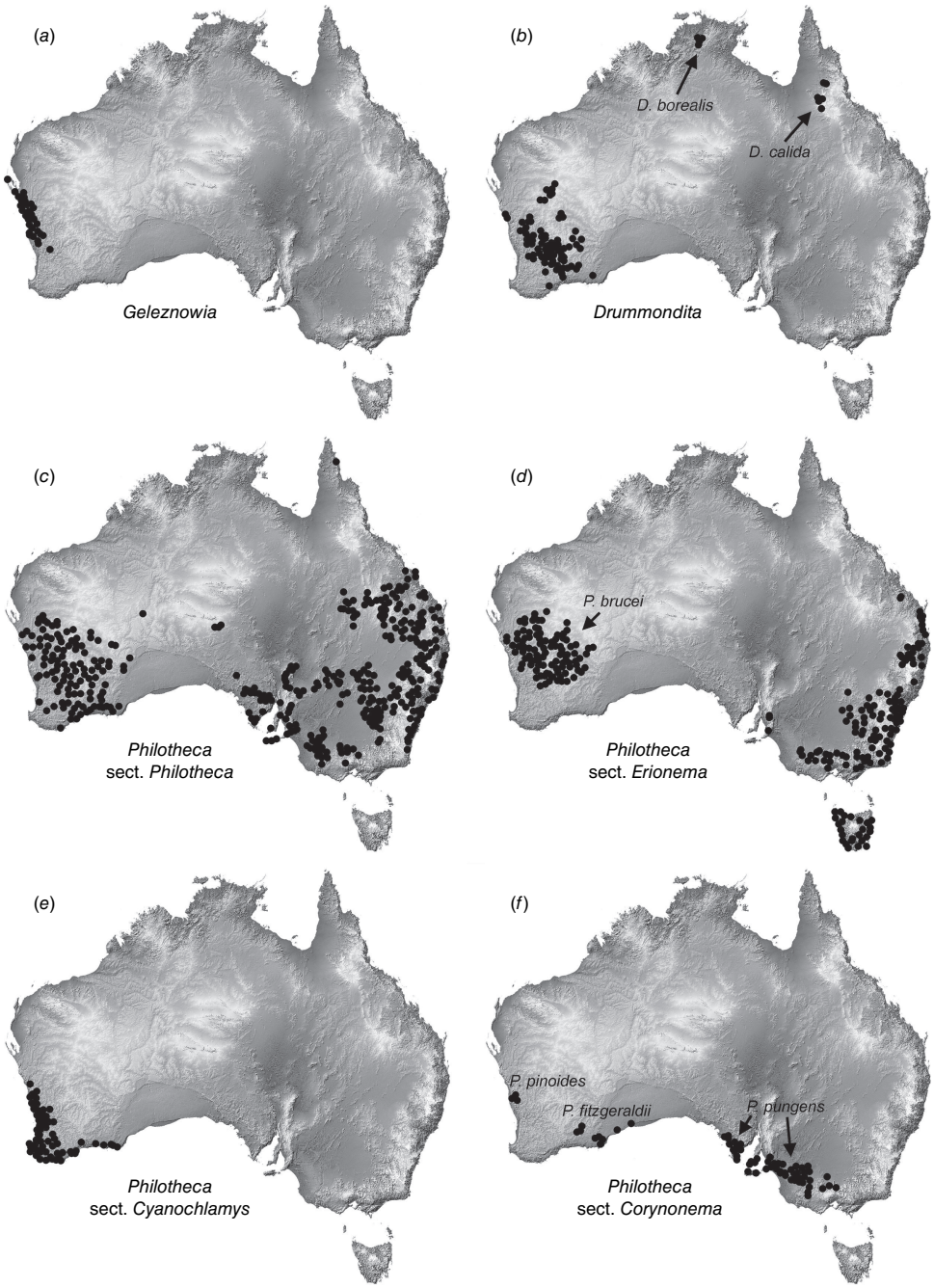

Fig. 1. Distributions of (*a*) *Geleznowia*, (*b*) *Drummondita*, (*c*) *Philotheca* section *Philotheca*, (*d*) *Philotheca* section *Erionema*, (*e*) *Philotheca* section *Cyanochlamys*, (*f*) *Philotheca* section *Corynonema*. Distributions are also indicated for (*b*) *D. borealis* and *D. calida* (the only species of *Drummondita* outside of Western Australia, (*d*) *P. brucei* (the only species of section *Erionema* in Western Australia, and (*f*) the three disjunct species comprising section *Corynonema*. Maps are based on filtered specimen records from The Australasian Virtual Herbarium (see https://avh.chah.org.au).

tubular flowers that are often red, orange, yellow or green on the petals, stamens or stigma (Fig. 2*b*, *c*), and that are bird pollinated (Armstrong 1987, 1991). The flowers of *Geleznowia* are bright yellow (to light green) and are unusual for the group in possessing petaloid bracts and sepals (Fig. 2*a*); the pollinator of these flowers is unknown (Armstrong 1979; Broadhurst and Tan 2001). Species in *Philotheca* section *Philotheca* possess comparatively unspecialised flowers that are most commonly white and open-petalled (Fig. 2*d*, *e*), although some are pendulous, tubular and more strongly coloured (Fig. 2*f*–*h*), and are pollinated variously by beetles, flies, bees, moths, butterflies, and birds (Armstrong 1979). The great degree of variance in derived morphological characteristics (i.e. highly specialised in *Drummondita* and *Geleznowia* *v*. largely unspecialised in section *Philotheca*) among *Philotheca* section *Philotheca*, *Drummondita* and *Geleznowia* means that classifying these taxa on the basis of morphology alone is unsatisfactory, owing to the fact that it is difficult to tell whether section *Philotheca* simply constitutes a group that is defined by symplesiomorphic characteristics. Because of this, further molecular phylogenetic investigation is necessary to clarify whether section *Philotheca* is monophyletic.

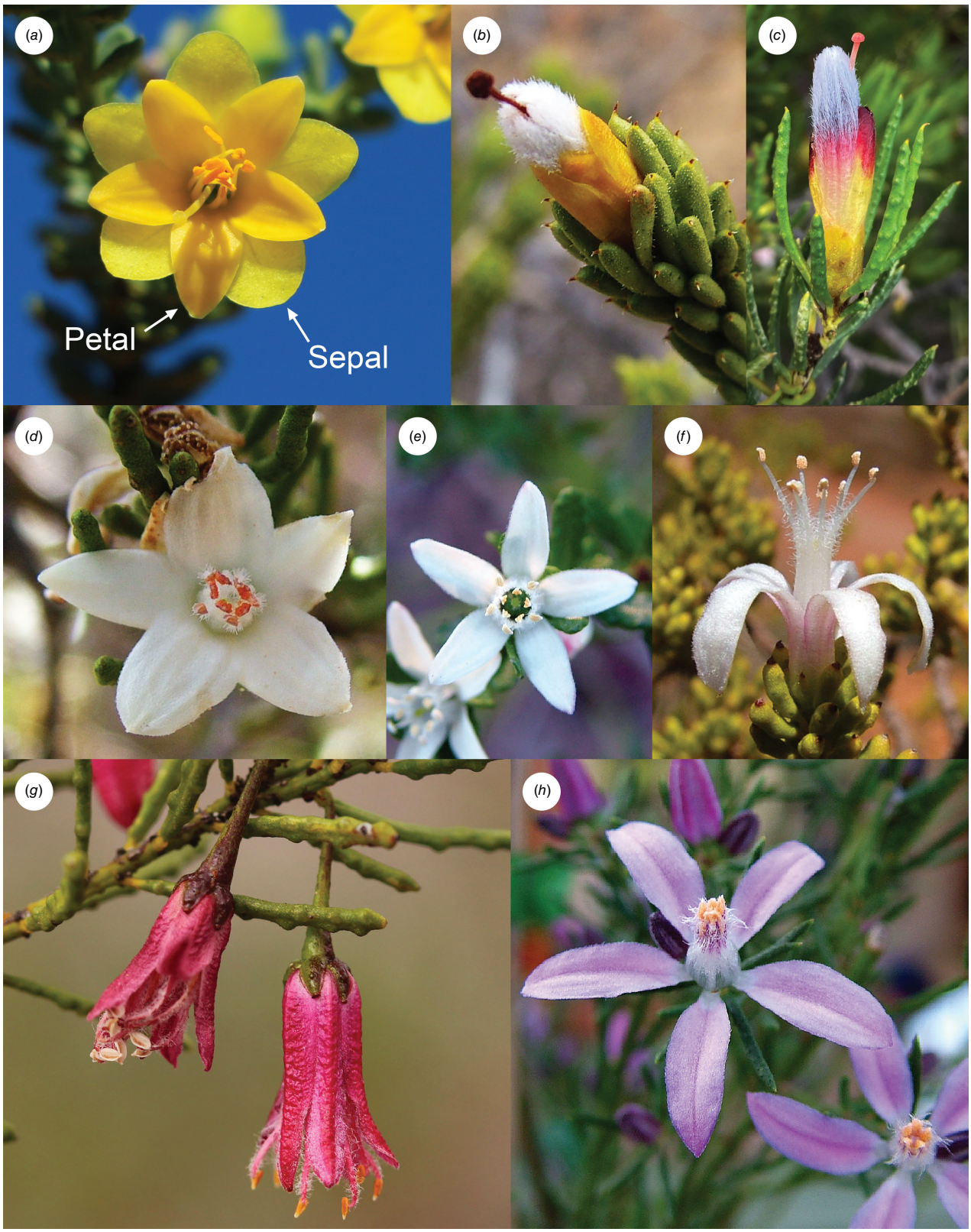

Fig. 2. Flowers of *Drummondita*, *Geleznowia* and *Philotheca* section *Philotheca*: (*a*) *Geleznowia verrucosa*, (*b*) *Drummondita hassellii*, (*c*) *D. longifolia*, (*d*) *Philotheca basistyla*, (e) *P. difformis* subsp. *smithiana*, (*f*) *P. tubiflora*, (*g*) *P. coccinea*, and (*h*) *P. salsolifolia*. Photographs: Michael Bayly.

Here, we seek to investigate phylogenetic relationships in the *Eriostemon* group by using a combination of genome-skimming sequence data and Sanger sequence data. In focussing on this group of taxa, our work expands on that of Mole *et al.* (2004), Bayly *et al.* (2013) and Duretto *et al.* (2023), with the aims of clarifying evolutionary relationships among genera, and testing the monophyly of genera, with particular focus on the genus *Philotheca*. Our approach represents a notable increase in the amount of taxon sampling and sequence data used to explore phylogenetic relationships in the group, which has previously been studied using only a low number of molecular markers.

Materials and methods

Taxon sampling and marker selection

To investigate relationships in the *Eriostemon* group, we generated complete plastome sequences for 67 accessions. We aimed to include multiple species from each Australian genus in the group. Two small Australian genera, *Geleznowia* (two species) and *Muiriantha* (one species), were each represented by collections of a single species. The New Caledonian genera *Neoschmidia* and *Myrtopsis* were also represented by single collections. For outgroups, we sampled members of the clade resolved as sister to the *Eriostemon* group by previous studies (Groppo *et al.* 2008; Bayly *et al.* 2013; Appelhans *et al.* 2021). This included species from the genera *Acronychia*, *Boronia*, *Brombya*, *Cyanothamnus*, *Euodia*, *Medicosma*, *Melicope*, *Neobyrnesia*, *Picrella* and *Zieria*. We included plastome sequence data for *Zanthoxylum simulans* Hance from Hou *et al.* (2018; GenBank accession number: NC037482) as a more distant outgroup, and with the addition of this taxon, our sampling of whole plastomes totalled 68 accessions (Table 1).

For a more detailed evaluation of relationships among *Philotheca*, *Drummondita* and *Geleznowia*, we generated Sanger sequence data for four plastome intergenic spacers (*psb*A–*trn*H, *rpl*32–*trn*L, *trn*L–*trn*F, *trn*Q–*rps*16) from an additional 22 species in this alliance (Table 1). These markers have been successfully used in other phylogenetic studies focussed on the Australian Rutaceae (e.g. Neal *et al.* 2019; Duretto *et al.* 2020). Information on the taxonomic coverage of our sampling across the *Eriostemon* group is provided in Table 2.

DNA extractions, library preparation and sequencing

DNA extractions for shotgun sequencing were performed following a modified CTAB protocol based on Shepherd and McLay (2011) by using ~25 mg of leaf tissue. DNA libraries for these samples were prepared 'in-house' following the protocol of Schuster *et al.* (2018). Libraries were sequenced on Illumina HiSeq 2000 (HiSeq SBS Kit, 2 × 125-bp paired-end reads) and Illumina NextSeq 550 (Mid-output kit, 2 × 150-bp paired-end reads) sequencing platforms at AgriBio, Centre for AgriBioscience (LaTrobe University) and the Walter and Eliza Hall Institute of Medical Research (WEHI) in Melbourne, Vic., Australia.

DNA extractions for Sanger sequencing from the additional samples of the *Philotheca* section *Philotheca*–*Drummondita*–*Geleznowia* alliance were performed on 25 mg of leaf tissue by using a DNeasy Plant Mini Kit (Qiagen), following the manufacturer's protocol, with a final elution volume of 100 µL. The *rpl*32–*trn*L, *trn*L–*trn*F and *trn*Q–*rps*16 regions were amplified from 10 to 20 ng of genomic DNA by following the method of Neal *et al.* (2019). The *psb*A–*trn*H region was amplified with psbAF (Sang *et al.* 1997) and trnH2 (Tate and Simpson 2003) primers, following the method of Duretto *et al.* (2020). Polymerase chain-reaction (PCR) products were purified following Neal *et al.* (2019) and sequenced at the Australian Genome Research Facility (AGRF) in Melbourne, Vic., Australia.

Sequence assembly, editing and alignment

Raw Illumina reads were *de novo* assembled into contigs with CLC Genomics Workbench (ver. 9.5.1, Qiagen) by using default settings. Contigs and raw reads were imported into Geneious Prime (ver. 2021.1.1, see http://www.geneious.com) and plastome sequences were assembled in this software. Initially, the plastome sequence of *Acronychia laevis* J.R.Forst. & G.Forst. was built using the plastome sequence of *Zanthoxylum schinifolium* Siebold & Zucc. (GenBank: NC030702) as a reference. To assemble full plastome sequences we adopted an approach of using a closely related, already-assembled plastome as the reference for the next assembly. For example, the assembled *Acronychia laevis* plastome sequence was used as a reference for the assembly of other closely related species (e.g. *Boronia imlayensis* P.H.Weston & Duretto, *Medicosma cunninghamii* (Hook.) Benth. & Hook.f., *Melicope hayesii* T.G.Hartley). Where they were more closely related to unassembled samples, these assemblies were then used as references for other plastome assemblies (e.g. *Boronia imlayensis* as the reference for *B. edwardsii* Benth. and *B. ternata* Endl.), and so on. Our assembly pipeline involved first mapping contigs to the selected reference by using custom sensitivity settings with three iterations, gaps allowed, *Maximum Per Read* set to 40% and *Maximum Gap Size* set to 1000. The resulting consensus sequence was exported, with any sites between contigs (i.e. with no contig coverage) called as the reference sequence. To replace reference sites and verify the draft sequence, the paired-end reads for the same sample were mapped to the consensus with three to five iterations, gaps allowed *Maximum Per Read* set to 40% and *Maximum Gap Size* set to 40. Reads mapped to the consensus were visually inspected for any erroneous mapping, with errors (such as poorly mapped reads at regions with mononucleotide

Table 1. Accession details for all samples.

Taxon name	Collector number	Herbarium voucher number(s)	GenBank number (full plastome)	GenBank numbers (Sanger)	Latitude	Longitude	Collection locality
Acronychia laevis	P.I.Forster 33410	BRI AQ0752244	OL591157	–	−25.93	152.1	Australia: Queensland, Grongah National Park.
Asterolasia asteriscophora	M.J.Bayly 2564	MELUD114862a	OL591158	–	−37.58	145.49	Australia: Victoria, Healesville.
Asterolasia drummondii	B.J.Mole 330	NSW 1003537	OL591159	–	−30.8	115.6	Australia: New South Wales.
Boronia edwardsii	M.J.Bayly 1974	MEL 2383596A	OL591160	–	−35.6	138.4	Australia: South Australia, Yankalilla.
Boronia imlayensis	M.J.Bayly 2005	MELUD105861a	OL591161	–	–	–	Australia: Cultivated, Australian National Botanic Garden (loc. 23a, Prop ID 749585).
Boronia ternata	M.J.Bayly 1931	MEL 2383603A	OL591162	–	−31.26	120.05	Australia: Western Australia, Boorabbin National Park.
Brombya platynema	P.I.Forster 34088	HO550407	OL591163	–	−17.58	145.7	Australia: Queensland, Wooroonooran National Park.
Chorilaena anceps	B.J.Mole 475	NSW 1003674	OL591221	–	−35.01	117.92	Australia: Western Australia, Albany.
Chorilaena euphemiae	B.J.Mole 424	NSW 1003630	OL591222	–	−33.99	122.14	Australia: Western Australia, Mount Le Grand.
Chorilaena quercifolia	M.J.Bayly 1954	MEL 2383575A	OL591164	–	−34.1	115.98	Australia: Western Australia, Netic State Forest.
Correa alba	M.J.Bayly 1876	MELUD105867a	OL591165	–	−38.4	144.18	Australia: Victoria, Anglesea.
Correa glabra	M.J.Bayly 2476	MELUD127019a	OL591166	–	−36.08	143.23	Australia: Victoria, Mount Wycheproof.
Correa lawrenceana var. *grampiana*	M.J.Bayly 1988	MEL 2383594A	OL591167	–	−37.29	142.59	Australia: Victoria, Grampians.
Correa lawrenceana var. *latrobeana*	M.J.Bayly 2567	MELUD114861a	OL591168	–	−37.53	145.51	Australia: Victoria, Toolangi.
Crowea angustifolia var. *platyphylla*	M.J.Bayly 1953	MEL 2383618A	OL591169	–	−34.58	116.4	Australia: Western Australia, Shannon National Park.
Crowea exalata subsp. *exalata*	D.J.Ohlsen *s.n.*	MELUD121723a	OL591170	–	−37.37	148.22	Australia: Victoria, W Tree.

(*Continued on next page*)

Table 1. (*Continued*)

Taxon name	Collector number	Herbarium voucher number(s)	GenBank number (full plastome)	GenBank numbers (Sanger)	Latitude	Longitude	Collection locality
Crowea exalata var. *revoluta*	M.J.Bayly 1992	MELUD105865a	OL591171	–	−36.67	144.25	Australia: Victoria, Greater Bendigo National Park.
Crowea saligna	D.J.Ohlsen *s.n.*	MELUD121722a	OL591172	–	−33.73	151.24	Australia: New South Wales, Sydney.
Cyanothamnus anemonifolius	M.J.Bayly 2562	MELUD114859a	OL591173	–	−37.74	144.31	Australia: Victoria, Brisbane Ranges National Park.
Diplolaena drummondii	M.J.Bayly 1956	MEL 2383571A	OL591174	–	−33.37	115.97	Australia: Western Australia, Wellington National Park.
Diplolaena obovata	M.J.Bayly 1908	MEL 2383570A	OL591175	–	−30.05	115.07	Australia: Western Australia.
Drummondita calida	P.I.Forster 22556	BRI AQ0605109	OL591176	–	−17.52	143.75	Australia: Queensland Bulleringa National Park.
Drummondita fulva	A.S.Markey 6212	MELUD105908a	OL591177	–	−29.1	116.9	Australia: Western Australia, Blue Hills Range.
Drummondita hassellii	M.J.Bayly 1925	MEL 2383612A	OL591178	–	−31.32	117.94	Australia: Western Australia, Trayning.
Drummondita hassellii	M.J.Bayly 1928	MEL 2383568A	–	OL660700; OM744163; OL660675; OL697857	−31.28	119.83	Australia: Western Australia, Yellowdine Nature Reserve.
Eriostemon australasius	P.I.Forster 34192	BRI AQ0743514	OL591179	–	−26.01	153.05	Australia: Queensland, Great Sandy NP.
Eriostemon banksii	P.I.Forster 33960	BRI AQ0743323	OL591180	–	−11.71	142.86	Australia: Queensland, Cape York Peninsula.
Euodia pubifolia	P.I.Forster 25751	BRI AQ0607159	OL591181	–	−16.14	145.43	Australia: Queensland, Daintree National Park.
Geleznowia verrucosa	B.J.Mole 344	NSW 1003545	OL591182	–	−29.99	115.91	Australia: Western Australia, Coorow.
Geleznowia verrucosa	M.J.Bayly 1910	MEL 2383587A	OL591183	–	−29.8	115.49	Australia: Western Australia, Tathra National Park.
Geleznowia verrucosa	M.J.Bayly 1909	MEL 2383586A	–	OL660701; OM744150; OM803177; OL697858	−29.8	115.49	Australia: Western Australia, Tathra National Park.
Halfordia kendack	D.G.Fell 10829	CNS 149723.1	OL591184	–	−10.18	142.23	Australia: Queensland, Moa Island.
Halfordia kendack	G.&N.Sankowksy 3019	MELUD105887a	OL591188	–	–	–	Australia: Cultivated Tolga. Arboretum number 276.

(*Continued on next page*)

Table 1. (*Continued*)

Taxon name	Collector number	Herbarium voucher number(s)	GenBank number (full plastome)	GenBank numbers (Sanger)	Latitude	Longitude	Collection locality
Halfordia kendack	P.I.Forster 34073	BRI AQ0743506	OL591185	–	−17.41	145.7	Australia: Queensland, Topaz.
Halfordia kendack	P.I.Forster 34090	BRI AQ0743446	OL591186	–	−17.45	145.48	Australia: Queensland, Herberton Range Forest Reserve.
Halfordia kendack	P.I.Forster 34580	BRI AQ0745524	OL591187	–	−12.25	143.09	Australia: Queensland, Cape York Peninsula.
Leionema beckleri	P.I.Forster 33439	BRI AQ0752479	OL591189	–	−28.22	153.21	Australia: Queensland, Lamington National Park.
Leionema ellipticum	P.I.Forster 25021	BRI AQ0606667	OL591190	–	−15.82	145.28	Australia: Queensland, Cedar Bay National Park.
Leionema lamprophyllum subsp. *obovatum*	M.J.Bayly 2563	MELUD114858a	OL591191	–	−37.74	144.31	Australia: Victoria, Brisbane Ranges National Park.
Leionema rotundifolium	P.I.Forster 34469	BRI AQ0745286	OL591192	–	−28.83	151.96	Australia: Queensland, Girraween National Park.
Medicosma cunninghamii	P.I.Forster 33501	BRI AQ0752476	OL591193	–	−26.45	152.97	Australia: Queensland, Sunshine Coast.
Melicope hayesii	P.I.Forster 36183	BRI AQ0813873	OL591194	–	−28.26	153.16	Australia: Queensland, Lamington National Park.
Muiriantha hassellii	B.J.Mole 474	NSW 1003673	OL591196	–	−34.4	118	Australia: Western Australia, Plantagenet.
Myrtopsis sp.	J.Munzinger 3458	NOU014250; MNHN-P-P04759709	OL591197	–	−22.1	166.64	New Caledonia: Riviére Bleu.
Nematolepis phebalioides	A.S.Markey 6215	MEL 2337320A; PERTH 8114846	OL591198	–	−33.66	120.28	Australia: Western Australia, Ravensthorpe Range.
Nematolepis squamea	P.I.Forster 34811	BRI AQ745513	OL591199	–	–	–	Australia: New South Wales, Wooyung, near Billinudgel.
Nematolepis wilsonii	M.J.Bayly 2568	MELUD114864a	OL591200	–	−37.83	144.98	Australia: Cultivated Royal Botanic Gardens Victoria.
Neobyrnesia suberosa	M.J.Bayly 1904	MEL 2383567A	OL591201	–	−12.44	132.97	Australia: Northern Territory, Kakadu National Park.

(*Continued on next page*)

Table 1. (*Continued*)

Taxon name	Collector number	Herbarium voucher number(s)	GenBank number (full plastome)	GenBank numbers (Sanger)	Latitude	Longitude	Collection locality
Neoschmidia pallida	P.H.Weston 3303	NSW783008	OL591202	–	–	–	New Caledonia: Cultivated Royal Botanic Garden Sydney, ex. Mount Dore.
Phebalium clavatum	B.J.Mole 398	NSW 1003609	OL591203	–	−31.2	121.3	Australia: Western Australia, Coolgardie.
Phebalium elegans	B.J.Mole 403	NSW 1003615	OL591204	–	−32.06	122.72	Australia: Western Australia, east of Norseman.
Phebalium longifolium	P.I.Forster 25088	BRI AQ0678653	OL591205	–	−17.32	145.42	Australia: Queensland, Mount Baldy State Forest.
Phebalium multiflorum	R.Butcher 1280	MELUD105904A; PERTH 8143110	OL591195	–	−33.66	120.27	Australia: Western Australia, Ravensthorpe Range.
Phebalium stenophyllum	M.J.Bayly 2560	MELUD127020a	OL591206	–	−36.61	141.75	Australia: Victoria, Little Desert.
Phebalium tuberculosum	B.J.Mole 375	NSW 1003583	OL591207	–	−31.48	118.33	Australia: Western Australia, east of Merridin.
Phebalium whitei	P.I.Forster 34467	BRI AQ0745285	OL591208	–	−28.83	151.96	Australia: Queensland, Girraween National Park.
Philotheca acrolopha	W.W.Cooper 2048	BRI AQ0745516; CNS 134918.1	–	OL660702; OM744164; OL660676; OL697859	−12.75	143.21	Australia: Queensland, Mount Tozer, Iron Range.
Philotheca angustifolia subsp. *angustifolia*	M.J.Bayly 1990	MEL 2383589A	OL591209	–	−36.55	144.35	Australia: Victoria, Greater Bendigo National Park.
Philotheca angustifolia subsp. *montana*	M.J.Bayly 1871	MELUD105857a	–	OL660703; OM744155; OL660677; OL697860	−36.88	142.37	Australia: Victoria, Mount Zero, northern Grampians.
Philotheca apiculata	M.J.Bayly 1939	MELUD105856a	–	OL660704; OM744147; OL660678; OL697861	−32.2	121.8	Australia: Western Australia.
Philotheca basistyla	M.J.Bayly 1924	PERTH 7810989	–	OL660705; OM744165; OL660679; OL697862	−31.3	118	Australia: Western Australia.
Philotheca brevifolia	M.J.Bayly 322	PERTH 7421087	–	OL660706; OM744167; OL660680; OL697863	−33.97	146.17	Australia: New South Wales, Cocoparra Nature Reserve.
Philotheca ciliata	P.I.Forster 29594	BRI AQ0647786; HO538812; NE 86281	–	OL660707; OM744168; OL660681; OL697864	−28.39	151.27	Australia: Queensland, Biggs Road, 18 km east of Inglewood.
Philotheca coateana	M.J.Bayly 1936	MELUD105855a	–	OL660708; OM744156; OL660682; OL697865	−29.2	120.1	Australia: Western Australia.

(*Continued on next page*)

Table 1. (*Continued*)

Taxon name	Collector number	Herbarium voucher number(s)	GenBank number (full plastome)	GenBank numbers (Sanger)	Latitude	Longitude	Collection locality
Philotheca coccinea	M.J.Bayly 1929	MEL 2383614A	–	OL660709; OM744149; OL660683; OL697866	−31.27	120.02	Australia: Western Australia, Boorabbin National Park.
Philotheca cuticularis	P.I.Forster 35315	BRI AQ0813977; MEL 2340118A	–	OL660710; OM744145; OL660684; OL697867	−25.71	144.46	Australia: Queensland, near Little Hell Hole Waterhole, Milo Station.
Philotheca deserti subsp. *deserti*	M.J.Bayly 1919	MEL 2383584A	–	OL660711; OM744144; OL660685; OL697868	−29.78	117.03	Australia: Western Australia, Great Northern Highway, 93.8 km south-west of Paynes Find.
Philotheca difformis subsp. *difformis*	M.T.Mathieson 274	MEL 2339553A	–	OL660712; OM744159; OL660686; OL697869	−26.11	147.64	Australia: Queensland, western end of 'Currawarra'.
Philotheca difformis subsp. *smithiana*	M.J.Bayly *s.n.*	MELUD121708a	OL591210	–	−26.41	152.98	Australia: Queensland, Tinbeerwah.
Philotheca ericifolia	M.J.Bayly 203	MEL 2278545A	–	OL660713; OM744161; OL660687; OL697870	−30.61	149.32	Australia: New South Wales, Pilliga East State Forest.
Philotheca fitzgeraldii	M.J.Bayly 1942	MEL 2383574A	OL591211	–	−32.63	121.55	Australia: Western Australia.
Philotheca gardneri	M.J.Bayly 1949	MEL 2383569A	OL591212	–	−33.46	119.99	Australia: Western Australia, Ravensthorpe.
Philotheca glabra	M.J.Bayly 1917	MEL 2383617A	–	OL660714; OM744146; OL660688; OL697871	−29.59	117.15	Australia: Western Australia, Great Northern Highway, 1 km south of White Wells turn-off.
Philotheca linearis	J.J.Bruhl 2864	NE 113630	–	OL660715; OM744157; OL660689; OL697872	–	–	–
Philotheca linearis	M.J.Bayly 186	MELUD105844a	–	OL660716; OM744158; OL660690; OL697873	−31.05	145.24	Australia: New South Wales, Beside Gidgee Road, 17.7 km west of Louth-Cobar Road.
Philotheca myoporoides subsp. *myoporoides*	M.J.Bayly 2565	MELUD114860a	OL591213	–	−37.53	145.52	Australia: Victoria, Toolangi.
Philotheca nodiflora subsp. *lasiocalyx*	M.J.Bayly 1962	MELUD105840a	OL591214	–	–	–	Australia: Cultivated ex. Kuranga.
Philotheca pachyphylla	M.J.Bayly 1932	MEL 2383619A	–	OL660717; OM744153; OL660691; OL697874	−31.04	120.84	Australia: Western Australia, 3.8 km west of Bullabulling on Great Eastern Highway.
Philotheca pinoides	M.J.Bayly 11	MELUD105845a	OL591215	–	−29.8	115.47	Australia: Western Australia, east of Eneabba.

(*Continued on next page*)

Table 1. (*Continued*)

Taxon name	Collector number	Herbarium voucher number(s)	GenBank number (full plastome)	GenBank numbers (Sanger)	Latitude	Longitude	Collection locality
Philotheca pungens	M.J.Bayly 1872	MELUD105849a	OL591216	–	−36.92	142.43	Australia: Victoria, Grampians.
Philotheca rhomboidea	M.J.Bayly 1950	MEL 2383576A	–	OL660718; OM744154; OL660692; OL697875	−33.36	119.87	Australia: Western Australia, Lake King-Ravensthorpe Road, near Lake Chidnup.
Philotheca salsolifolia subsp. *salsolifolia*	M.J.Bayly 1961	MELUD105841a	–	OL660719; OM744169; OL660693; OL697876	–	–	Australia: Victoria, Cultivated in Rosanna.
Philotheca sericea	M.J.Bayly 1916	MEL 2383579A	–	OL660720; OM744151; OL660694; OL697877	−29.29	117.48	Australia: Western Australia, ~20 km west-south-west of Paynes Find.
Philotheca spicata	M.J.Bayly 1907	MEL 2383588A	OL591217	–	−30.07	115.53	Australia: Western Australia.
Philotheca sporadica	M.T.Mathieson 217	MEL 2339573A	–	OL660721; OM744160; OL660695; OL697878	−27.07	150.84	Australia: Queensland, Condamine Highway, east of Kogan.
Philotheca thryptomenoides	M.J.Bayly 1921	MEL 2383582A	–	OL660722; OM744162; OL660696; OL697879	−29.78	117.03	Australia: Western Australia, Great Northern Highway 93.8 km south-west of Paynes Find.
Philotheca tomentella	M.J.Bayly 1913	MEL 2383616A	OL591218	–	−28.44	116.04	Australia: Western Australia, Pindar.
Philotheca trachyphylla	M.J.Bayly 1900	MELUD105850a	OL591219	–	−37.73	148.09	Australia: Victoria, Nowa Nowa.
Philotheca tubiflora	M.J.Bayly 1934	MELUD105854a	–	OL660723; OM744152; OL660697; OL697880	−28.3	122.6	Australia: Western Australia.
Philotheca verrucosa	M.J.Bayly 2199	MELUD121711a	–	OL660724; OM744166; OL660698; OL697881	−37.89	144.22	Australia: Victoria, Brisbane Ranges.
Philotheca virgata	M.J.Bayly 266	MELUD105843a	–	OL660725; OM744148; OL660699; OL697882	−37.4	149.26	Australia: Victoria, Coopracambra National Park, Mount Kaye walking track.
Picrella glandulosa	M.J.Bayly 2104	MEL 2383678A	OL591220	–	−20.32	164.42	New Caledonia: Province Nord.
Zanthoxylum simulans	**see Hou *et al.* (2018)**	**NC037482**					
Zieria arborescens subsp. *arborescens*	M.J.Bayly 2566	MELUD114863a	OL591223	–	−37.53	145.51	Australia: Victoria, Toolangi.

Genbank numbers for Sanger sequences are listed in the order: *psb*A–*trn*H; *rpl*32–*trn*L; *trn*L–*trn*F; *trn*Q–*rps*16. Samples included from previous existing sequences on GenBank are in bold.

Table 2. Taxonomic coverage of sampling from the *Eriostemon* group.

Genus	Section	Number of species sampled (full plastome data)	Number of species sampled (Sanger data)	Total number of species
Asterolasia		2		19
Chorilaena		3		4
Correa		3		11
Crowea		3		3
Diplolaena		2		15
Drummondita		3	(1)	11
Eriostemon		2		2
Geleznowia		1	(1)	2
Halfordia		1		1–3
Leionema		4		28
Muiriantha		1		1
Myrtopsis		1		~9
Nematolepis		3		7
Neoschmidia		1		2
Phebalium		7		38
Philotheca	*Corynonema*	3		3
	Cyanochlamys	2		2
	Erionema	2	2	15
	Philotheca	4	20 (2)	34
Total		48	22 (4)	~206–209

Numbers in parentheses indicate where the same species was sampled in both the full plastome and Sanger datasets. Total number of species includes described taxa only (i.e. phrase-named species are excluded).

repeats) being corrected manually. We then exported the read-mapped consensus using a site consensus threshold of 75% (i.e. sites with <75% consensus were treated as ambiguities) and sites with coverage of less than three reads were treated as *N* values (unidentified nucleotides). The plastome sequence of *Neoschmidia pallida* T.G.Hartley was found to possess significant structural rearrangements and differed substantially from any other plastome sequences in our dataset. Because of this, we used the 'get_organelle_from_reads.py' script of GetOrganelle (ver. 1.7.5.3, see https://github.com/Kinggerm/GetOrganelle; Jin *et al.* 2020) to assemble a draft plastome of that accession. This draft plastome was then treated in the same manner as were the other initial exported consensuses (following the contig-mapping step) to produce a final plastome sequence. Across all samples, the mean number of reads mapped to the final plastome sequence of each sample was 148 418, with an average read depth of 140 reads per sample (individual statistics provided in Supplementary Table S1). Owing to frequent shifting of gene boundaries across taxa preventing the accurate transfer of annotations between plastome sequences, we batched annotated plastomes by using GeSeq (see https://chlorobox.mpimp-golm.mpg.de/geseq.html; Tillich *et al.* 2017) with default annotators. Annotations were then manually checked, corrected and *N*s were annotated as GenBank features by using a custom Python script.

Following assembly, we opted to split plastome sequences into individual loci, rather than align whole plastome sequences for increased alignment accuracy. For this process, we used a workflow that employed several steps in Geneious to extract protein-coding sequences (CDS) and non-coding spacer loci. tRNA and rRNA sequences were excluded because of the often short length and low variability of these loci. For CDS loci, introns were removed (~13 000 bp per sample) and exons concatenated. Non-coding spacer loci were extracted, aligned, and sites with more than 30% gaps were removed to prevent the inclusion of non-homologous sites, and loci were then extracted from the alignment file to individual sequence files. For loci present in both inverted repeat regions of the plastome, the copy from inverted repeat B was removed. In total, 41 loci with fewer than 62 sequences were removed, and the remaining 183 CDS and spacer loci were aligned separately using MAFFT (ver. 7.450, see https://mafft.cbrc.jp/alignment/software/; Katoh *et al.*

2002; Katoh and Standley 2013) with default settings. Individual locus alignments were manually checked for errors and two alignments were removed owing to poor quality (the *ndh*A–*ndh*H spacer, being an alignment of a single base; the *rps*3–*rpl*22 spacer, with sequences of varying lengths owing to this locus traversing an inverted repeat boundary in some taxa). The alignments were then concatenated and, to reduce the potential for inclusion of non-homologous sites, sites with more than 80% gaps were removed to produce a final 'phylogenomic' alignment of the 68 samples that was 106 885 base pairs in length (65 778 bp CDS, 41 107 bp non-coding).

In addition to the plastome assemblies, we also assembled the complete *18S–5.8S–26S* nuclear ribosomal cistron from the genome-skimming data. These sequences were intended to be analysed to test for cytonuclear discordance and assess genetic relationships, but the resulting phylogeny was poorly supported overall and results are largely not discussed here owing to the equivocality of most branches in the tree. The methods and results of analysis of the nuclear ribosomal cistron sequences are presented in the 'Methods and results of analyses of *18S–5.8S–26S* nuclear ribosomal cistron sequences from shotgun-sequenced samples' section of the Supplementary material (hereafter the Supplementary 'Methods and results' section).

Several studies have shown that phylogenetic resolution of Sanger sequence datasets can be improved by integrating them with phylogenomic datasets (e.g. Bardon *et al.* 2016; Williams *et al.* 2016; Hammer *et al.* 2019). The integration of these different types of data can be undertaken either at the alignment stage, with Sanger data sequences appended to large-scale alignments to form a 'supermatrix', or by analysing the datasets separately and running phylogenetic analyses of Sanger data under a constrained topology resolved by the genomic dataset. Preliminary tests of both methods on our data found that the supermatrix approach produced a better-resolved and more highly supported tree than did the constrained topology approach, a result also found by Williams *et al.* (2016). Hence, we opted to use the supermatrix approach to investigate relationships in *Philotheca*, *Drummondita* and *Geleznowia*. Sanger sequences were edited in Sequencher (ver. 4.10.1, Gene Codes Corporation) and imported into Geneious. Sanger sequence regions *psb*A–*trn*H, *rpl*32–*trn*L, *trn*L–*trn*F and *trn*Q–*rps*16 were aligned with the same spacer regions as taken from the complete plastomes, and sites with more than 30% gaps were removed to account for potentially non-homologous alignment sites. The four integrated locus alignments were concatenated with the remaining plastome-derived locus alignments to produce a final 'supermatrix' alignment of 94 samples that was 106 714 base pairs in length. Complete plastome and Sanger sequences were deposited in GenBank (Table 1).

Phylogenetic analyses

We analysed the phylogenomic alignment by using maximum likelihood and Bayesian inference approaches in IQ-TREE (ver. 2.1.3, see http://www.iqtree.org/; Minh *et al.* 2020*b*) and MrBayes (ver. 3.2.7a, see https://nbisweden.github.io/MrBayes/download.html; Ronquist *et al.* 2012) under three partition schemes: (1) unpartitioned, (2) coding (CDS) *v*. non-coding sequences and (3) partitioned by codon position and coding *v*. non-coding sequences. We also ran an IQ-TREE analysis, with the data partitioned by locus. To check for possible site saturation, we translated the CDS locus alignments to amino acids and analysed them with IQ-TREE, comparing the resulting phylogeny with those produced from DNA alignments. To estimate branch support across our IQ-TREE analyses, we employed default ultrafast bootstrap (UFBoot) (Hoang *et al.* 2018) and SH-aLRT (Guindon *et al.* 2010), with each being set to 1000 replicates. For these analyses, best-fit models were estimated in IQ-TREE using ModelFinder (see http://www.iqtree.org/ModelFinder/; Kalyaanamoorthy *et al.* 2017). For the Bayesian analyses, the '-mset' option was used to restrict model searches to those implemented in MrBayes. Information on partitioning and model selection is provided in Supplementary Table S2. MrBayes analyses were run for 1 000 000 generations with a 25% burn-in; we manually checked that the standard deviation of split frequencies was below 0.01 by the end of each run. Following this, we assessed convergence in Tracer (ver. 1.7.2, see http://beast.community/tracer; Rambaut *et al.* 2018) to ensure that effective sample sizes were above 200 for all parameters. To evaluate our data further, we produced gene trees for all loci with IQ-TREE and used these as input for coalescent analysis in ASTRAL-III (ver. 5.7.7, see https://github.com/smirarab/ASTRAL; Zhang *et al.* 2018), inferring local posterior probability as support values. We also used the option '−t 10' to test for possible hard polytomies in the species tree (Sayyari and Mirarab 2018). In addition, we used the individual locus alignments and gene trees to calculate concordance factors for the phylogeny produced under the unpartitioned scheme in IQ-TREE, following the method of Minh *et al.* (2020*a*); this approach calculates site concordance (sCF: the fraction of decisive alignment sites supporting a branch in the species tree) and gene concordance (gCF: the proportion of gene trees that are concordant with any particular branch in the species tree).

On the basis of results from analyses of the phylogenomic alignment (in which partitioning did not affect topology – see Results), we analysed the supermatrix alignment with IQ-TREE and MrBayes following the same approach as used for analyses of the phylogenomic alignment, with data treated as unpartitioned.

Investigating a polytomy in the backbone of the *Eriostemon* group

The phylogenetic analyses described above all produced phylogenetic trees with a large polytomy along the backbone of the *Eriostemon* group. To further investigate this polytomy, we performed additional analyses with the aim of

assessing potential causes of the polytomy and increasing phylogenetic resolution.

Exploration of phylogenetic tree space

Previous studies have found that analysis of phylogenetic tree space can improve phylogenetic resolution and low branch support by accounting for topological discordance among loci (Duchêne *et al.* 2018; Foster *et al.* 2018). To investigate topological congruence across gene trees in the full-plastome dataset we followed the methods of Duchêne *et al.* (2018) and Foster *et al.* (2018), with some modifications. Loci with incomplete sampling (i.e. $n < 68$) were removed to avoid topological differences owing to missing tips, for a total of 148 input loci (71 CDS, 77 non-coding spacers; further details are provided in Supplementary Table S3). Gene trees were estimated using maximum likelihood in RAxML (ver. 8.2.11, see https://github.com/stamatak/standard-RAxML; Stamatakis 2014), assuming a GTR + GAMMA substitution model with rapid bootstrapping and 100 replicates. We used the R package treespace (ver. 1.1.4.1, see https://cran.r-project.org/package=treespace; Jombart *et al.* 2017) to calculate unweighted Robinson–Foulds pairwise distances (Penny and Hendy 1985) between all pairs of trees generated with RAxML. We used the R package CLUSTER (ver. 2.1.4, M. Maechler, P. Rousseeuw, A. Struyf, M. Hubert and K. Hornik, see https://CRAN.R-project.org/package=cluster) to calculate the optimal number of clusters (k) by using the gap statistic (Tibshirani *et al.* 2001) for $k_{max} = 16$. Gene trees were separated on the basis of this optimal cluster number, and phylogenetic trees for each cluster were generated in ASTRAL. To further assess the topology of each cluster, the individual locus alignments were separated on the basis of the optimal cluster number, concatenated, and analysed in IQ-TREE.

Likelihood mapping analysis

To assess phylogenetic discordance and noise in our data, we used likelihood mapping (Strimmer and von Haeseler 1997) to estimate measures of tree-like, net-like and star-like evolution supported by each locus in the phylogenomic dataset for all 183 loci. Likelihood mapping was conducted in IQ-TREE by using the 'lmap' function with 5000 randomly drawn quartets, and scores for basins of attraction (where Regions 1, 2, 3 support tree-likeness; Regions 4, 5, 6 support net-likeness; Region 7 supports star-likeness) were evaluated for each locus alignment. To minimise the contribution of net-like and star-like topologies, locus alignments were then grouped into three subsets on the basis of percentage of fully resolved quartets (i.e. tree-likeness) at minimum values of 50, 60 and 70%. Maximum-likelihood phylogenies for each of these subsets were generated in IQ-TREE and branch support was estimated using UFBoot and SH-aLRT values with 1000 replicates. For this, alignments were automatically concatenated and analysed using the '$-p$' option (to partition by locus). We also manually concatenated the alignments of each subset and viewed these as a NeighbourNet (Bryant and Moulton 2002) phylogenetic network in SplitsTree (ver. 4.17.0, see https://software-ab.cs.uni-tuebingen.de/download/splitstree/welcome.html; Huson and Bryant 2006) under default parameters (i.e. using uncorrected P distances and equal-angle splits).

Topology testing

To test support for the various possible resolutions of the polytomy, we conducted tree-topology tests. The maximum-likelihood (ML) tree produced from the phylogenomic alignment partitioned by locus was read into *R*, and all possible topological resolutions for the polytomy node were generated with the 'resolveNodes' function of the package phytools (ver. 1.0-3, see https://github.com/liamrevell/phytools; Revell 2012). We also generated an additional hard polytomy topology (i.e. truly multifurcating) by collapsing the short unsupported branches that formed the polytomy in the ML tree. To account for the potential influence of branch lengths on topology scores, all trees were treated as cladograms with branches set to a length of one. Topology tests were then run on this set of trees in IQ-TREE, by using the '$-zw$' option to calculate log-likelihoods, estimating model parameters with '$-n$ 1', and conducting the bootstrap proportion test, unweighted and weighted Kishino–Hasegawa (Kishino and Hasegawa 1989) and Shimodaira–Hasegawa tests (Shimodaira and Hasegawa 1999), expected likelihood weights test (Strimmer and Rambaut 2002) and approximately unbiased test (Shimodaira 2002) by using 100 000 RELL (Kishino *et al.* 1990) replicates.

Results

Analyses of plastome data (phylogenomic alignment)

The phylogenomic alignment included 30 038 variable sites, of which 16 845 were parsimony informative (Table 3). Across all phylogenetic analyses of the phylogenomic alignment, no

Table 3. Alignment Information.

Item	Number of variable sites	Number of parsimony-informative sites	Number of constant sites	Total length (bp)
Phylogenomic alignment	30 038	16 845	76 847	106 885
Supermatrix alignment	30 057	16 895	76 657	106 714

supported topological incongruence was recovered (Supplementary Fig. S1). The IQ-TREE analyses produced identical topologies and similar branch support across all partition schemes. The MrBayes analyses produced topologies with no supported incongruence. Across all analyses, and consistent with previous findings (Bayly *et al.* 2013; Appelhans *et al.* 2021), we found high support (posterior probability (PP): 1, UFBoot (UFB): 100, SH-aLRT (SH): 100) for the *Eriostemon* group, with *Neoschmidia* and *Halfordia* as the first successive divergences from the rest of the clade (see Fig. 3). Relationships in the *Eriostemon* group were mostly well resolved and fully supported, with the exception of a series of extremely short branches (coloured red on Fig. 3), effectively forming a polytomy in the backbone of the group in all analyses. The MrBayes and IQ-TREE phylogenies recovered four supported clades branching from this polytomy (see Fig. 3): Clade 1, including *Drummondita*, *Geleznowia*, *Philotheca* section *Philotheca* and *Philotheca* section *Erionema*; Clade 2, including *Muiriantha* and *Philotheca* section *Cyanochlamys*; Clade 3, including *Correa*, *Leionema* and *Myrtopsis*; Clade 4, including *Asterolasia*, *Chorilaena*, *Crowea*, *Diplolaena*, *Eriostemon*, *Nematolepis*, *Phebalium* and *Philotheca* section *Corynonema*. We note that topology of the MrBayes tree was slightly different from that of the IQ-TREE, with Clades 2–4 being resolved as a polytomy (hence the missing support value ('−') in Fig. 3) in an unsupported clade (PP: 0.53); but the low support for this clade still effectively rendered Clades 1–4 as a polytomy.

The phylogeny produced with ASTRAL recovered five supported clades branching from the polytomy, differing from the MrBayes and IQ-TREE phylogenies in lacking support for the unification of *Eriostemon* and its allies (Clade 4A in Fig. 3; *Crowea*, *Philotheca* section *Corynonema*) with *Phebalium* and its allies (Clade 4B in Fig. 3; *Asterolasia*, *Diplolaena*, *Chorilaena*, *Nematolepis*) (see Clade 4, Fig. S1). The ASTRAL polytomy test did not reject the null hypothesis that the backbone polytomy should not be treated as a true polytomy (Supplementary Fig. S2: $P > 0.05$ for all branches) and did not reject the collapsing of the branch uniting the *Eriostemon* alliance (i.e. Clade 4 A) and *Phebalium* alliance (i.e. Clade 4B) ($P = 0.629$). Concordance factors for the branch uniting the two Clade 4 alliances in the unpartitioned phylogenies are low, but all other support values are high (Fig. 3).

Within Clade 1, *Philotheca* section *Erionema* was resolved as sister to other members with high support (PP: 1, UFB: 100, SH: 100). *Drummondita* was placed sister to *Geleznowia* and *Philotheca* section *Philotheca* with high support, and *Geleznowia* and *Philotheca* section *Philotheca* were resolved as sister to each other with high support.

Clade 2 was resolved on a highly supported long branch, with *Muiriantha* sister to *Philotheca* section *Cyanochlamys*.

In Clade 3, *Myrtopsis* was placed sister to *Correa* and *Leionema* with high support. The monophyly of *Correa* and of *Leionema* was highly supported.

The largest clade, Clade 4, was resolved with high posterior probability and bootstrap support, but low gene and site concordance (PP: 1, UFB: 100, SH: 99.9, gCF: 4.92, sCF: 35). We found high support for a clade (Fig. 3, 4*a*) comprising *Crowea*, *Eriostemon* and *Philotheca* section *Corynonema*. *Crowea* was resolved as polyphyletic, with the two eastern Australian species, *C. exalata* and *C. saligna*, placed sister to the rest Clade 4A with high support. *Crowea angustifolia*, the sole western Australian species of the genus, was resolved sister to *Eriostemon* on a long branch with high support, and together this clade was placed sister to a monophyletic *Philotheca* section *Corynonema* with high support. The other taxa of Clade 4 (*Asterolasia*, *Chorilaena*, *Diplolaena*, *Nematolepis*, *Phebalium*) constitute a group that has been historically referred to as the *Phebalium* group (Wilson 1998*b*; Mole *et al.* 2004). In our analyses, these genera formed a well-supported clade (Fig. 3, 4*b*) that was placed sister to Clade 4A. Within the *Phebalium* group, *Asterolasia* was resolved as sister to the rest of the group with high support. *Diplolaena* was found to be sister to the remaining genera with high support. Also with high support, *Nematolepis* was resolved sister to *Chorilaena*. *Phebalium* was resolved sister to the clade of *Chorilaena* and *Nematolepis* with high support.

Analyses of combined plastome and Sanger data (supermatrix alignment)

The supermatrix alignment included 30 057 variable sites and 16 895 parsimony-informative sites (Table 3). The topologies recovered in both the IQ-TREE and MrBayes phylogenies were consistent with those produced by analyses of the phylogenomic alignment. No supported topological incongruence was present across the IQ-TREE and MrBayes phylogenies. The additional samples represented by Sanger sequence data in the supermatrix dataset were all placed in Clade 1 (i.e. with *Philotheca* section *Erionema*, *Drummondita*, *Geleznowia*, and *Philotheca* section *Philotheca*; see Fig. 4). As the supermatrix and phylogenomic alignment phylogenies differ only in Clade 1, the IQ-TREE phylogeny built from the supermatrix alignment (Fig. 4) is presented, with emphasis on relationships in Clade 1.

In Clade 1 *Philotheca* section *Erionema* was strongly supported as monophyletic and sister to all other taxa. *Philotheca* section *Philotheca* was recovered as polyphyletic, with *P. coateana* Paul G.Wilson, *P. sericea* (Paul G.Wilson) Paul G.Wilson, *P. tubiflora* A.S.George, *P. basistyla* Mollemans, *P. acrolopha* Paul G.Wilson, *P. salsolifolia* (Sm.) Druce and *P. ciliata* Hook. placed in a well-supported clade with *Drummondita*. The other members of *Philotheca* section *Philotheca* formed a highly supported clade sister to *Geleznowia*. The single, but poorly supported, topological difference between the IQ-TREE and MrBayes phylogenies was the position of *Philotheca angustifolia* within section *Philotheca* (PP: 0.99 *v*. UFB: 63; indicated in Fig. 4).

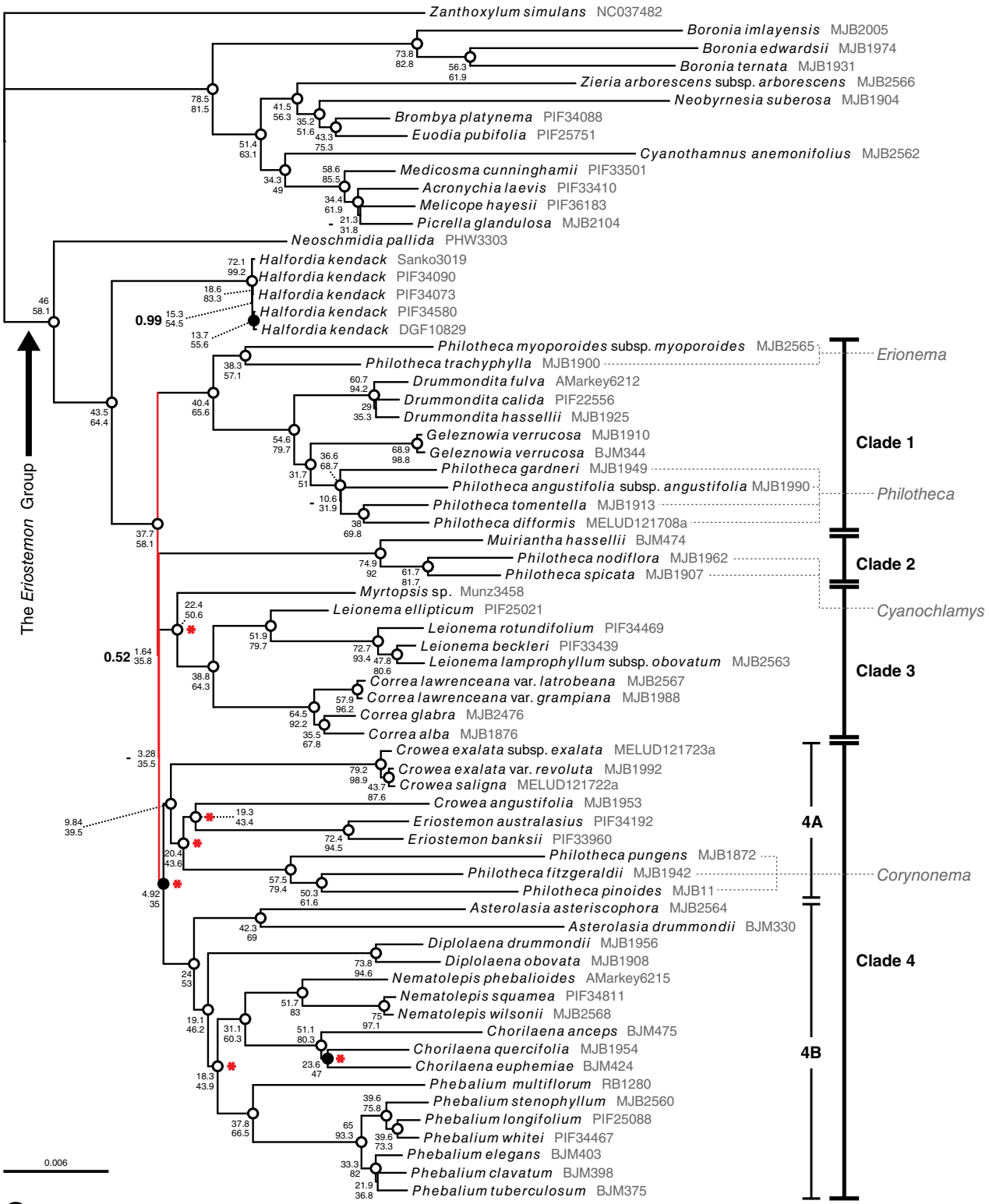

Fig. 3. (*Caption on next page*)

Fig. 3. Maximum-likelihood phylogeny of the *Eriostemon* group produced from IQ-TREE analysis of the unpartitioned 'phylogenomic' alignment of samples with full plastome data. UFboot and SH-aLRT support for branches are denoted by dots at nodes, where open circles denote 100% UFboot and 100% SH-aLRT support and closed circles denote 100% UFboot and <100% SH-aLRT support, and no dot present on the node indicates <100% for both metrics. Concordance factors are provided next to node dots, with gene concordance (gCF) positioned above site concordance (sCF). Posterior probabilities from the MrBayes 50% majority-rule consensus tree are superimposed to the left of the concordance factors in bold type at nodes where branch support is not maximal (i.e. <1; dashes occur where a branch was non-existent in the MrBayes tree). Short, unsupported branches that effectively form a polytomy in the backbone of the tree are coloured red. Red asterisks at nodes indicate branches that are well supported in our phylogeny but were unsupported in the plastid sequence phylogeny of Duretto *et al.* (2023). Sections of *Philotheca* are listed in grey, and are linked to corresponding taxa by dashed lines.

Investigation of the *Eriostemon* group polytomy

Analysis of tree space

Our approach identified the optimal number of gene tree clusters in our data as three. Cluster 1 contained 72 loci (33 protein-coding, 39 non-coding) with a mean length of 955 bp, and a mean number of parsimony-informative sites of 141. Cluster 2 contained 50 loci (21 protein-coding, 29 non-coding) with a mean length of 276 bp, and a mean number of parsimony-informative sites of 44. Cluster 3 contained 26 loci (17 protein-coding, 9 non-coding) with a mean length of 378 bp, and a mean number of parsimony-informative sites of 66. Re-estimating the phylogeny for each of the three clusters produced trees with no supported incongruence between, for both IQ-TREE (Supplementary Fig. S3) and ASTRAL phylogenies (see files under Data availability). RAxML gene trees from Clusters 1 and 2 were significantly longer than those in Cluster 3 (Dunn's test; Bonferroni adjusted $P = 8.99 \times 10^{-6}$ and $P = 5.52 \times 10^{-4}$ respectively; Supplementary Fig. S4). Bootstrap support was significantly different among all clusters, with support values in Cluster 1 being markedly higher than those in Clusters 2 and 3 (Dunn's test; Bonferroni adjusted $P = 2.97 \times 10^{-13}$ for C1–C2, $P = 2.31 \times 10^{-21}$ for C1–C3, $P = 1.87 \times 10^{-3}$ for C2–C3; Fig. S4).

Likelihood-mapping analysis

Across all loci, the mean percentage of fully resolved quartets (i.e. quartets falling into Regions 1, 2 and 3 of the likelihood-mapping plot) was 53%. The means for partly resolved quartets (Regions 4, 5 and 6) and unresolved quartets (Region 7) were 4 and 43% respectively. The subset of loci with >50% fully resolved quartets contained 102 loci with a mean length of 851 bp, and a mean number of parsimony-informative sites of 140. The subset of loci with >60% fully resolved quartets contained 63 loci with a mean length of 1056 bp, and a mean number of parsimony-informative sites of 178. The subset of loci with >70% fully resolved quartets contained 22 loci with a mean length of 1490 bp, and a mean number of parsimony-informative sites of 302.

Phylogenetic analysis of each of the subsets resulted in trees with identical topologies that were congruent with the phylogeny produced in the analysis of the unpartitioned full dataset (i.e. Fig. 3). In general, all subset trees had slightly lower branch support than the full-dataset tree. Among subset trees, the >70% tree had the lowest branch support, with exception to the placement of *Philotheca angustifolia* sister to *P. tomentella* and *P. differmis* with low-to-moderate support (UFBoot: 91; SH-aLRT: 82.9). The >50 and >60% trees did not resolve the position of this species. Despite the removal of potentially noisy or discordant loci, none of the subset trees contained a supported resolution for the backbone polytomy; the >60% subset tree displayed the highest support for short branches of the polytomy, but these branches were still unsupported and resulted in star-like resolution of the polytomy in our network analysis (Fig. 5*b*). We found a significant difference in the number of resolved quartets between the three gene tree clusters from the tree space analysis (one-way ANOVA test; $F(2,145) = 18.82$, $P = 5.39 \times 10^{-8}$; Kruskal–Wallis rank sum test; $H = 40.437$, d.f. = 2, $P = 1.657 \times 10^{-9}$). The mean number of resolved quartets for Clusters 1, 2 and 3 was 3019 ($\sigma = 586$), 2434 ($\sigma = 541$) and 2213 ($\sigma = 1030$) respectively, indicating that Cluster 1 contained the most phylogenetically informative loci on average.

Tree topology tests

Owing to high UFBoot and posterior probability support for four clades forming the backbone polytomy, our tree-topology testing investigated support for the 15 possible relationships among these clades (Fig. 6*a*). Log-likelihood values for each topology ranged from −494 970.83 to −494 975.48. Expectedly, the topology of the most likely tree used as input was found to have the highest log-likelihood (−494 970.83); this topology was identical to the 15th possible resolution of the polytomy (Fig. 6*a*). Five topologies were found to have slightly higher log-likelihoods than the others (Fig. 6*b*: Topologies 15, 5, 10, 13, 14). The three most likely topologies (15, 5, 10) were the only topologies to resolve the Clade 1 sister to the rest of the group. Clades 1 and 2 were grouped sister to Clades 3 and 4 in Topology 13, and in Topology 14 Clade 2 was sister to the rest of the group, with Clade 1 being sister to Clades 3 and 4. The AU test rejected four topologies ($P < 0.05$): 7, 9, 12 and the hard polytomy. The hard polytomy was found to be one of the least likely topologies, having a low log-likelihood score (−494 975.27) and being statistically supported by

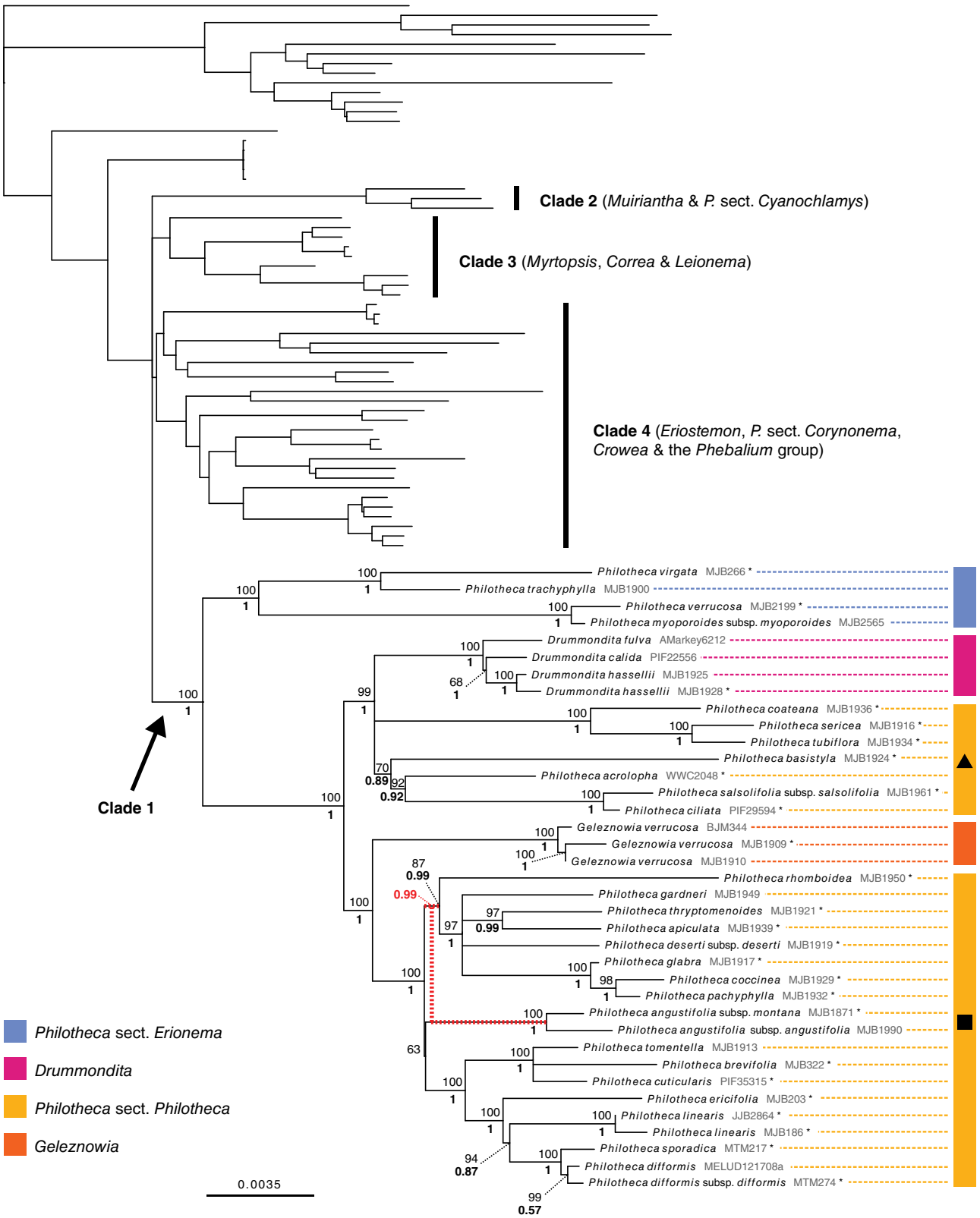

Fig. 4. (*Caption on next page*)

Fig. 4. Phylogenetic relationships in Clade 1. Maximum-likelihood phylogeny produced from IQ-TREE analysis of the 'supermatrix' alignment of combined full plastome and Sanger sequences. UFboot support for branches is positioned above posterior probabilities from the MrBayes 50% majority-rule consensus tree of the same dataset. Relationships in other clades are identical to those in Fig. 3. Unsupported short branches in the backbone of the *Eriostemon* group have been manually collapsed to a polytomy. Asterisks denote samples represented only by Sanger sequence data. The MrBayes and IQ-TREE phylogenies differed in the placement of *Philotheca angustifolia*; this incongruence is shown by red-dashed branches that indicate the topology recovered by MrBayes (posterior probability value relevant to this is in red). Black triangle, *Philotheca* s.str. (largely equivalent to *Philotheca sensu* Wilson 1971); black square, *Philotheca 'Nigrostipulae'* (largely equivalent to *Eriostemon* section *Nigrostipulae sensu* Wilson 1970), as discussed in the text.

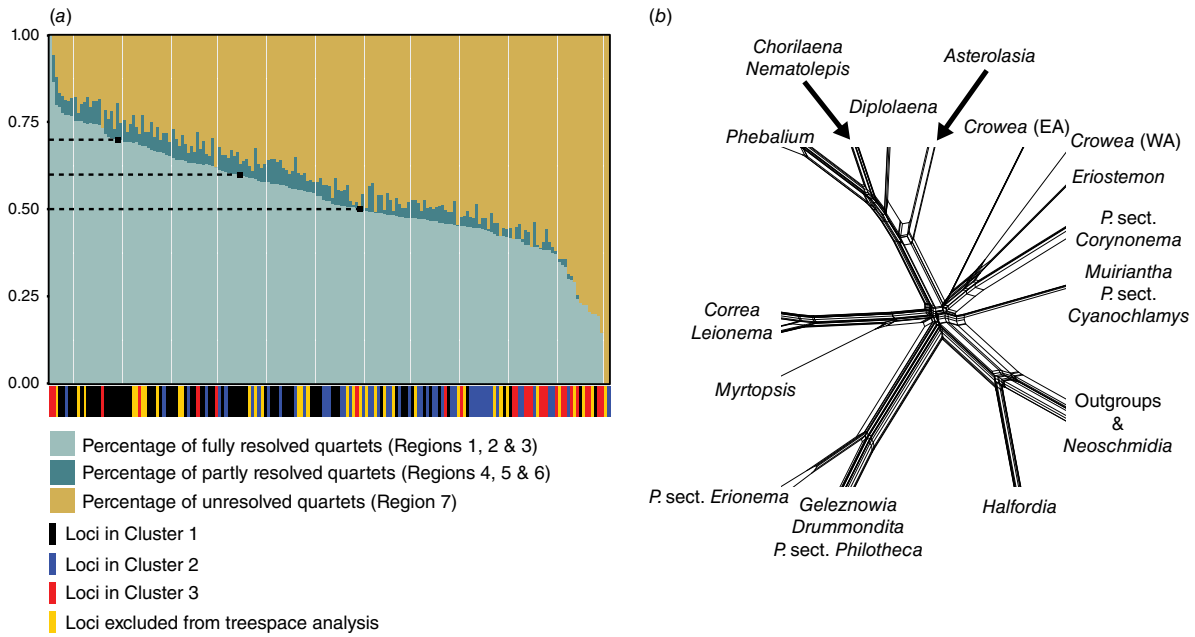

Fig. 5. Results of the likelihood-mapping analysis of loci. (*a*) Plot of phylogenetic informativeness of individual loci, where a higher percentage of fully resolved quartets for a locus indicates greater support for tree-like evolution. Dashed lines on the plot indicate the three cut-off values that were tested for potentially improving phylogenetic resolution of the polytomy (i.e. 50, 60 and 70%). Bars along the *x*-axis denote the cluster that each locus was placed in during the analysis of tree space; some loci were excluded from the tree-space analysis, owing to incomplete representation of samples. (*b*) Phylogenetic network (NeighborNet) showing splits of the backbone polytomy; constructed from a concatenated alignment of all loci with >60% of quartets fully resolved. For *Crowea*, EA, eastern Australia; WA, western Australia.

only the unweighted and weighted SH tests ($P = 0.225$ and $P = 0.648$), which did not reject any topologies (*P*-values greater than 0.05 for all topologies). The bootstrap proportion and equal likely weights test did not place the hard polytomy topology in the 95% confidence set of trees. Summary statistics from topology testing are provided as Supplementary Table S4.

Discussion

Generic relationships in the *Eriostemon* group

The current study was conducted concurrently with a similar study by Duretto *et al.* (2023), who also investigated relationships in the *Eriostemon* group. Duretto *et al.* (2023) focussed primarily on relationships in the *Phebalium* group (Clade 4B in our analyses) and *Leionema*, sampling comprehensively across those genera by using five markers (5145 bp in total; plastid markers *psb*A–*trn*H, *trn*L–*trn*F, *rbc*L; nrDNA markers *ITS*, *ETS*). With their smaller genetic dataset but more thorough taxon sampling of the group, they confirmed the monophyly of *Asterolasia*, *Diplolaena*, *Leionema*, *Nematolepis* and *Phebalium* (Duretto *et al.* 2023). This is congruent with our results, although our sampling of these genera is not appropriate for commenting on their monophyly. The results of our analyses are mostly congruent with those of Duretto *et al.* (2023) and support the taxonomic changes made by those authors, namely, the transfer of *Rhadinothamnus* (=*C. anceps* and *C. euphemiae* in our analyses) to *Chorilaena*, and *Microcybe* (=*P. multiflorum* in our analyses) to *Phebalium*. Our larger genetic

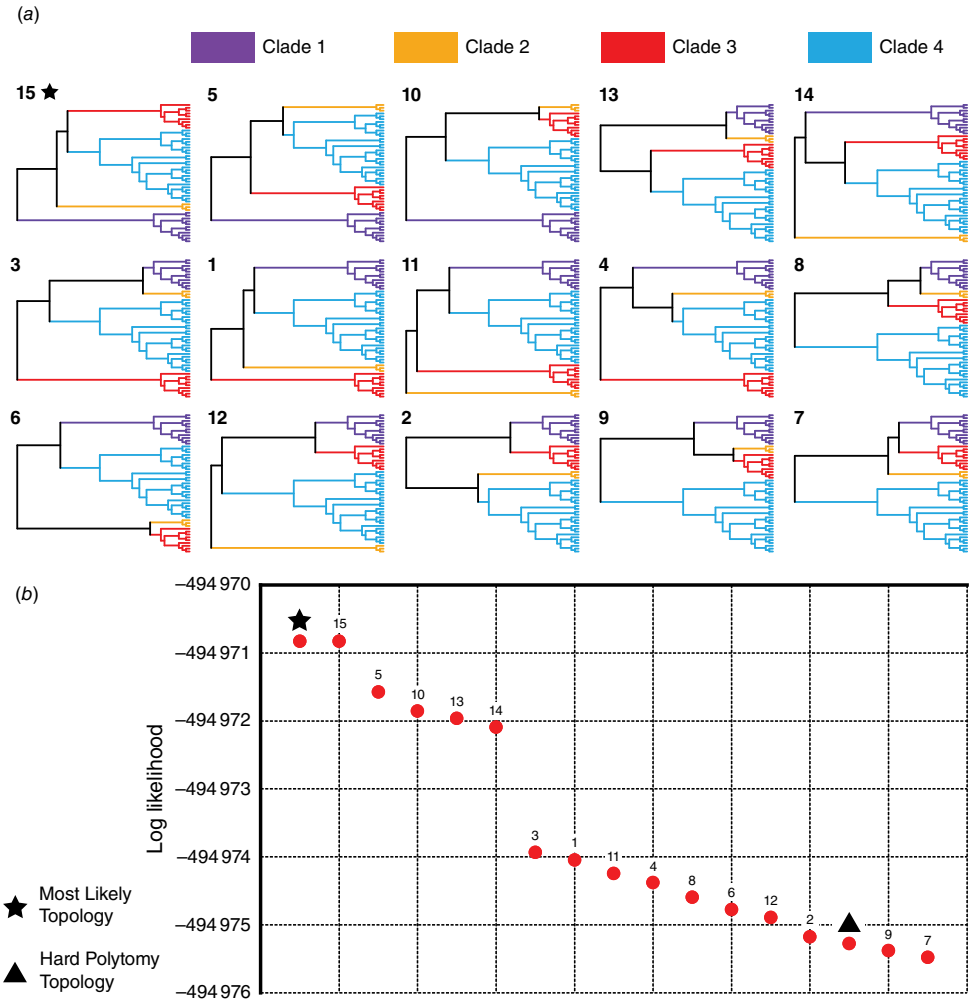

Fig. 6. Results of topology tests for the backbone polytomy in the *Eriostemon* group. (*a*) The 15 possible resolutions of the polytomy (for the four supported clades) that testing was conducted on, ordered by most likely to least likely from left to right, top to bottom (note: the hard polytomy resolution is not depicted). (*b*) Plot of log likelihoods for each possible topology. The topology matching the most likely tree is denoted by a star, and the hard polytomy topology is denoted by a triangle.

dataset has further clarified relationships among some genera by providing maximal support for branches previously unresolved (<0.95 PP in the ptDNA phylogeny of Duretto *et al.* 2023; indicated on Fig. 3). The following sections discuss some relationships, supported here, that are noteworthy; relationships in the *Phebalium* group are not discussed here because they have already been thoroughly discussed by Duretto *et al.* (2023).

Relationships of *Myrtopsis*, *Correa* and *Leionema*

We provide high support for a clade of *Correa*, *Leionema* and *Myrtopsis*, three genera that previous studies have been unable to confidently place (Bayly *et al.* 2013; Appelhans *et al.* 2021); this group was recovered as an unsupported clade by Duretto *et al.* (2023). This clade contains probably the most varied morphological characters in the *Eriostemon* group. The recovery of a sister relationship between *Leionema* and *Correa* is congruent with the plastid sequence phylogeny of Duretto *et al.* (2023) and is of note because the two genera differ vastly morphologically. *Correa* is unique in the *Eriostemon* group in possessing consistently 4-merous flowers that are mostly tubular and bird-pollinated (except for *C. alba* Andrews, which is nested among bird-pollinated species) (Armstrong 1979; French *et al.* 2016). Although bird pollination occurs in other taxa (e.g. some *Leionema*, *Nematolepis* and *Philotheca*), the flowers of all other genera in the group are 5-merous (with the exception of *Philotheca virgata* (Hook.f.) Paul G.Wilson). *Correa* is also distinct in possessing leaves that are oppositely arranged, although this feature also occurs in *Myrtopsis*. All other members of the *Eriostemon* group have alternate leaves. Consequently, the order of relationships among *Correa*, *Leionema* and *Myrtopsis* that we have recovered, (*Myrtopsis* (*Correa*, *Leionema*)), implies either a single transition to opposite

leaves at the stem of the clade and a subsequent reversal to alternate leaves in *Leionema*, or separate independent transitions to opposite leaves in *Myrtopsis* and *Correa*. The placement of the New Caledonian endemic *Myrtopsis* firmly within the *Eriostemon* group is consistent with several previous studies (Bayly *et al.* 2013; Appelhans *et al.* 2021; Baker *et al.* 2022; Duretto *et al.* 2023).

Historically, the relationship of *Myrtopsis* with other genera of Austral-Pacific Rutaceae has been difficult to deduce from morphology. On the basis of morphological cladistic analyses, Armstrong (1991) resolved the genus as sister to the *Eriostemon* group (minus *Correa*, which was placed in the *Boronia* clade), although this placement was equivocal owing to limited availability of plant material. This contrasted with Hartley (1995), who considered *Myrtopsis* most closely related to *Boronella* Baill. (=*Boronia* Sm.), *Euodia*, *Brombya* and *Medicosma*, and separated the genus from the rest of tribe Boronieae on the basis of embryo shape and cotyledon width. Certain elements of the distinct morphology of *Myrtopsis* could be related to adaptation to New Caledonian habitats with nutrient-poor, ultramafic soils and comparatively higher temperatures and humidity than in the southern half of Australia, where the majority of species in the *Eriostemon* group occur.

The presence of *Myrtopsis* only in New Caledonia is interesting biogeographically. Evidence exists for possible land connections between Australia and New Caledonia into the Paleocene and Eocene ~60–35 million years ago (Ladiges and Cantrill 2007), meaning that a vicariance explanation cannot be ruled out should the divergence of *Myrtopsis* pre-date this. Time-calibrated phylogenies have tentatively estimated the divergence of *Myrtopsis* from the Oligocene to the mid-Miocene ~30–15 million years ago (Bayly *et al.* 2013; Joyce *et al.* 2023), implicating long-distance dispersal to New Caledonia from Australia after re-emergence of the main island during the Paleocene–Eocene (37 ± 3 million years ago; Grandcolas 2017). This is in line with the crown ages of most New Caledonian clades across the tree of life (Nattier *et al.* 2017). However, Bayly *et al.* (2013) stated that their divergence-date estimates should be treated with caution because of a limited availability of fossils within Rutaceae for calibration; they highlighted that trial analyses conducted with fewer fossil calibrations had the effect of producing much younger age estimates. Hence, the divergence of *Myrtopsis* in that estimation may appear younger than it should, and a vicariance explanation for the split should not yet be discounted on the basis of the current understanding of phylogenetic relationships and lack of consensus from divergence-dating analyses.

Relationships of *Crowea*, *Eriostemon* and *Philotheca* section *Corynonema*

The placement of *Crowea*, *Eriostemon* and *Philotheca* section *Corynonema* in a highly supported clade (Clade 4A), together with strong support for relationships in that clade, improved on previous understanding of the ptDNA relationships of these taxa. Duretto *et al.* (2023) also resolved these three taxa in a well-supported clade in two of their analyses, but found somewhat conflicting relationships between the taxa according to different datasets; they found weak support for a sister relationship between *Eriostemon* and *Crowea* in their combined nrDNA–ptDNA phylogeny, weak support for a sister relationship between *Philotheca* section *Corynonema* and *Crowea* in their ptDNA phylogeny, and the taxa were not resolved in a clade in their nrDNA phylogeny. We have not identified obvious morphological synapomorphies that unite all three groups, but several morphological studies have proposed a sister relationship between *Crowea* and *Eriostemon* that is incongruent with our placement of *Eriostemon* (and *Crowea angustifolia* Sm.; see next paragraph for discussion of that species) as sister to *Philotheca* section *Corynonema* (Armstrong 1991; Bayly 2001). *Crowea* and *Eriostemon* differ from the rest of the *Eriostemon* group in having petals with at least three main veins (rather than one main vein) originating from their base (Bayly 2001). Armstrong (1991) also considered *Crowea* and *Eriostemon* united by staminal filaments that are arranged pyramidally over the ovary at anthesis, although this was questioned by Bayly (2001), who argued that the feature is not as striking in *Eriostemon*, and that staminal arrangement in *Eriostemon* is not dissimilar to some species of *Philotheca* (=*Eriostemon* section *Nigrostipulae* Paul G.Wilson). In addition, chromosome numbers for *Crowea* ($n = 19$) and *Eriostemon* ($n = 17$) are unique in the *Eriostemon* group, where n is most commonly 14 (*Asterolasia*, *Geleznowia*, *Drummondita*, *Muiriantha*, *Philotheca* sectin *Philotheca*, *P.* section *Erionema*, *P.* section *Cyanochlamys*, some *Diplolaena*) or 16 (*Correa*, *Leionema*, *Nematolepis*, *Phebalium*) (Smith-White 1954; Armstrong 1991; Stace and Armstrong 1992; Bayly 2001). Chromosome numbers for species in *Philotheca* section *Corynonema* are unknown, and future cytological investigation of this group would provide valuable insight into how well the cytology of this section aligns with *Crowea* and *Eriostemon*.

Our recovery of *Crowea* as polyphyletic in ptDNA analyses is perhaps not surprising. Duretto *et al.* (2023) found support for the monophyly of *Crowea* to vary between nrDNA and plastid datasets, with ptDNA suggesting that the genus may be non-monophyletic because of the only western Australian species, *C. angustifolia* (using different accessions to the current study), forming a polytomy with the eastern Australian *Crowea* and *Eriostemon*. Our results have improved the clarity of ptDNA relationships in this group and confirmed that ptDNA suggests *Crowea* is non-monophyletic with the placement of *C. angustifolia* as sister to *Eriostemon* with high support. However, our phylogenetic analyses of nrDNA sequences (see the Supplementary 'Methods and results' section) mirror the findings of Duretto *et al.* (2023) and suggest the genus is monophyletic. Such cytonuclear discrepancy may arise from one, or a combination of, incomplete lineage sorting (ILS), horizontal gene transfer and organellar genome

capture (Rieseberg and Soltis 1991; Tsitrone *et al.* 2003; Toews and Brelsford 2012). Given that both *Eriostemon* species occur only in eastern Australia, it is unlikely that their sister placement to *C. angustifolia* in ptDNA trees is the result of the last two processes, as they require gene flow between the genera (or their common ancestors) to occur; on the basis of the current distribution of taxa, it is simpler to infer that there has been no historical reconnection between *C. angustifolia* and *Eriostemon*, rather than infer that there has been exclusive connectivity between the two (across the whole of Australia) in the absence of gene flow with the other species of *Crowea*. Although we cannot rule out the latter scenario, we feel a more likely explanation involves ILS of the plastome of *C. angustifolia*, because this matches the simpler scenario outlined above and is consistent with ILS having a greater influence on plastid markers due to larger effective population sizes, and thus longer coalescence times than for nrDNA markers that are subject to concerted evolution (Buckler and Holtsford 1996; Clowes *et al.* 2022). Further work is required to deduce the cause of this discordance.

Relationships of *Philotheca* section *Cyanochlamys* and *Muiriantha*

The placement of *Philotheca* section *Cyanochlamys* sister to *Muiriantha* in Clade 2 is consistent with the findings of Duretto *et al.* (2023). These taxa are quite distinct from each other morphologically, and were speculatively thought to be allied to *Philotheca* (for *P.* section *Cyanochlamys*) and the *Phebalium* group (for *Muiriantha*) on morphological grounds (Wilson 1970). The only species of *Muiriantha*, *M. hassellii* (F.Muell.) C.A.Gardner, and both species of *P.* section *Cyanochlamys*, *P. spicata* (A.Rich.) Paul G.Wilson and *P. nodiflora* (Lindl.) Paul G.Wilson, are endemic to south-western Australia, so this relationship is geographically sensible. *Muiriantha hassellii* has pendulous flowers with imbricate yellowish-green petals that form an elongated tube (Fig. 7*a*), whereas the flowers of *Philotheca* section *Cyanochlamys* are borne erectly, with petals spreading and ranging from pink to blue in colour (Fig. 7*b*, *c*).

On the basis of Duretto *et al.* (2023) and our nrDNA analyses (see the Supplementary 'Methods and results' section), it is apparent that the close relationship of *Philotheca* section *Cyanochlamys* and *Muiriantha* is consistent across nrDNA and ptDNA. However, in contrast to our ptDNA results, our analyses of nrDNA resolved *Muiriantha* nested inside *P.* section *Cyanochlamys*, with very high support (see the Supplementary 'Methods and results' section). Duretto *et al.* (2023) found the same discrepancy in the position of *Muiriantha* between ptDNA and nrDNA datasets, but the nesting of *Muiriantha* in *P.* section *Cyanochlamys* in their nrDNA phylogeny was not well supported.

Despite obvious morphological differences between *Philotheca* section *Cyanochlamys* and *Muiriantha*, they are broadly similar in having a subshrub habit and leaves with a somewhat papery texture. Further morphological examination by the authors has also shown similarities in carpel surfaces and branchlet indumenta (Fig. 7).

In *Muiriantha* and *P.* section *Cyanochlamys*, the abaxial surface of the carpels is conspicuously pitted with small glands (Bayly 2001; Fig. 7*d–f*). This feature is otherwise known only in *Philotheca pinoides* (section *Corynonema*) (Bayly 2001) and is, therefore, considered apomorphic for *Muiriantha* and section *Cyanochlamys* in the context of major clades of the *Eriostemon* group.

In *Philotheca* section *Cyanochlamys*, two types of branchlet hairs are found (Bayly 2001). The first type is long (~0.6 mm), silky, distally ascending and somewhat appressed, and is fasciculate (having multiple hairs arising from a single base) but not spreading; these hairs are always present in *P. nodiflora*, and are sometimes absent in *P. spicata*. The second type is fasciculate–stellate, with multiple hairs arising from a single base that spread out in a stellate manner, and occurs in both species of *P.* section *Cyanochlamys* (Bayly 2001). *Muiriantha* also possesses two types of hairs; the first is similar to the long, silky, appressed hairs of *P.* section *Cyanochlamys*, but differs in being singular (i.e. one hair, not multiple from a single base), the second is fasciculate hairs that are the same as those of *P.* section *Cyanochlamys*. Fasciculate hairs of this type (Fig. 7*g–i*) are an apparent synapomorphy for Clade 2, as they do not occur in any other members of the *Eriostemon* group.

Finally, from comparing descriptions of *Philotheca* sections *Cyanochlamys* and *Muiriantha* (Wilson 1970, 2013*a*, 2013*b*), it is apparent that seed features between these taxa are superficially similar. Preliminary investigations of seeds in these taxa by the authors has confirmed that they share a subreniform shape, linear hilum and sub-basal raphe, but it remains unclear whether these characteristics are synapomorphic or plesiomorphic. More detailed investigations of seed morphology may clarify whether or not these similar features should be treated as synapomorphic, and provide further characters that could be used to assign these taxa to a morphologically diagnosable taxonomic group (e.g. subtribe).

Relationships of *Philotheca* section *Erionema*, *P.* section *Philotheca*, *Drummondita* and *Geleznowia*

Our well-supported recovery of Clade 1, containing *Philotheca* section *Erionema*, *P.* section *Philotheca*, *Drummondita* and *Geleznowia*, is consistent with results of Duretto *et al.* (2023), and was also recovered with low support by Appelhans *et al.* (2021). Within this clade, the monophyly and divergence of *Philotheca* section *Erionema*, placed as sister to the other taxa, is supported by several morphological synapomorphies (Bayly 2001; Batty *et al.* 2022), including anther and seed characters. In particular, the seeds of *P.* section *Erionema* are unique in the *Eriostemon* group and readily recognisable in being ellipsoid and laterally flattened with a linear hilum on the adaxial

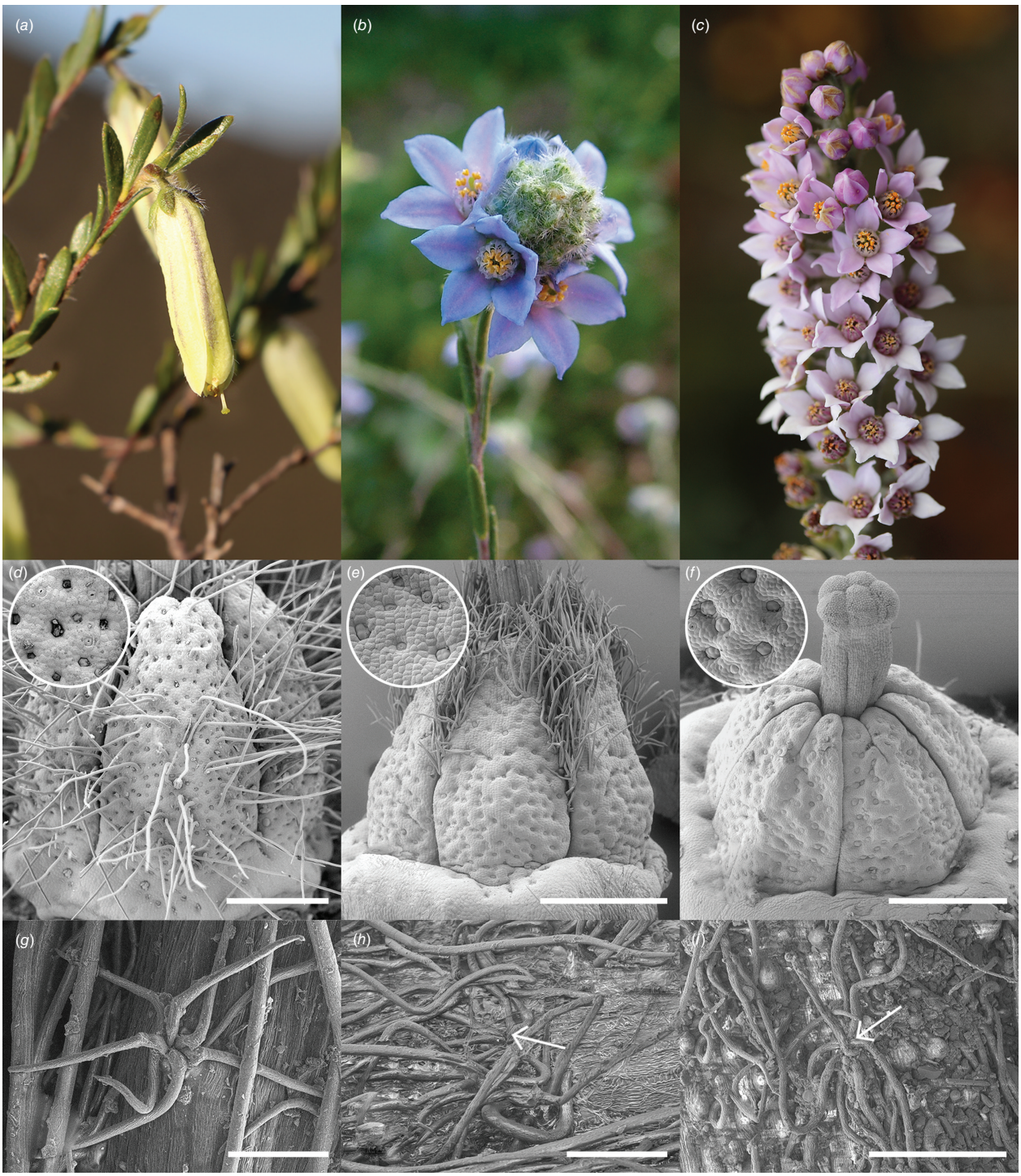

Fig. 7. Flowers, carpels (with pitted surfaces), and fasciculate stem hairs of *Muiriantha* and *Philotheca* section *Cyanochlamys* (voucher numbers indicated in brackets): (*a*, *d*, *f*) *Muiriantha hassellii* [*MJB 2574*, MELUD155083a], (*b*, e, *h*) *Philotheca nodiflora* subsp. *lasiocalyx* [*b*, e, *MJB 108*, MELU; *h*, *MJB 1962*, MELUD105840a], (*c*, *f*, *i*) *Philotheca spicata* [c, *f*, *MJB 9*, MELU; *i*, *MJB 10*, MELU]. Scale bars: 500 μm, in micrographs of carpels (inset close-up images of pits are not to scale), and 100 μm, in micrographs of hairs (arrows indicate fasciculate hairs in *h*, *i* that are obscured by other hairs).

face and having a basal raphe and chalazal region (Fig. 8; Wilson 1998*a*; Bayly 2001). In contrast, seeds of *Philotheca* section *Philotheca*, *Drummondita* and *Geleznowia* (Fig. 8), which share a strong morphological resemblance in comparison to other members of the *Eriostemon* group, are more or less reniform, substantially thicker than their length, have a

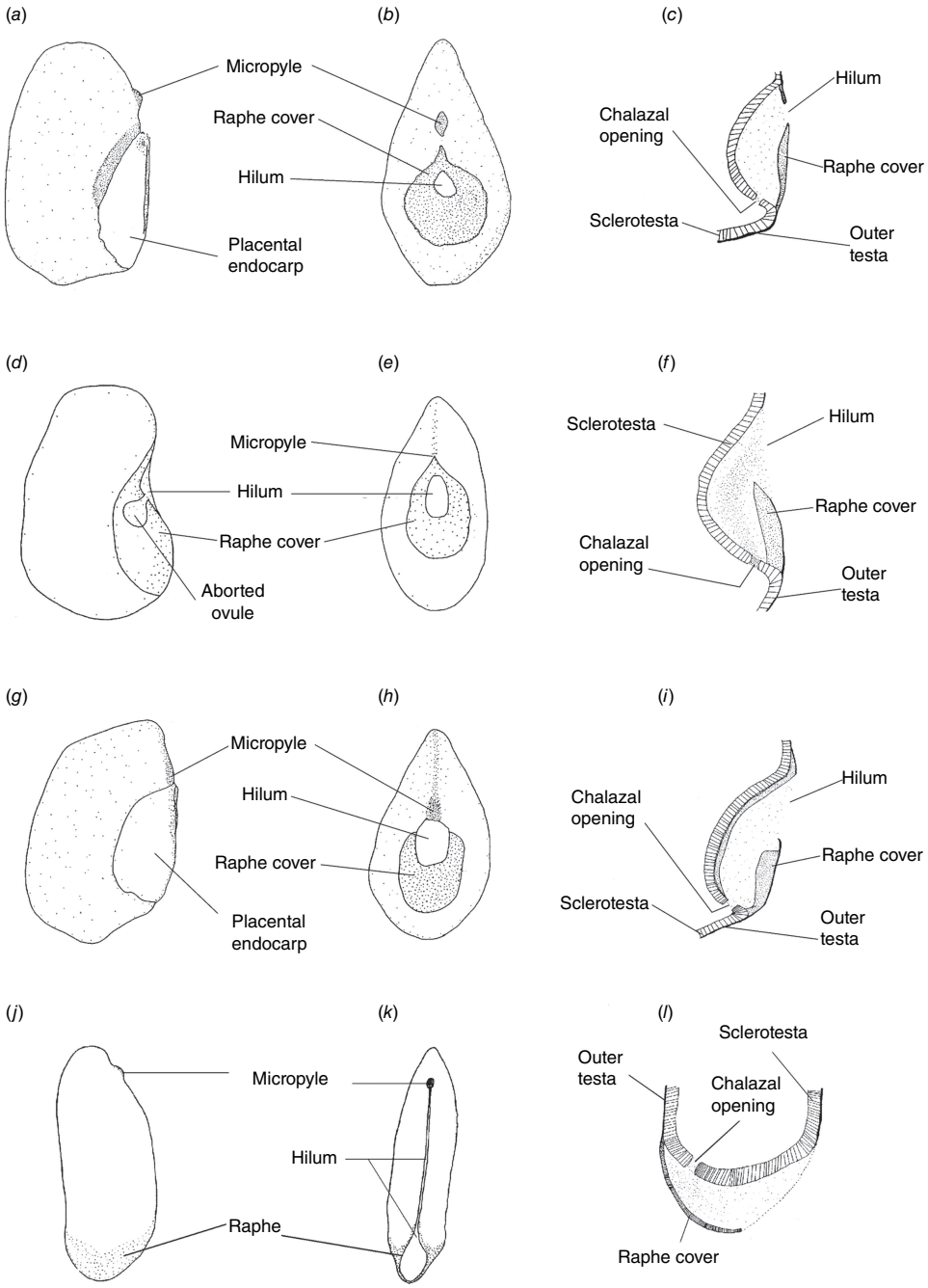

Fig. 8. Seed morphology in Clade 1, showing the adaxially central raphe in *Philotheca* section *Philotheca*, *Drummondita* and *Geleznowia*, and the basal raphe in *Philotheca* section *Erionema*. (*a*–*c*) Seeds typical of *P.* section *Philotheca* [*P. linearis*; *G.J. White s.n.*, NE 52727]. (*d*–*f*) Seeds typical of *Drummondita* [*D. longifolia*; *H. Demarz 10361*, PERTH 959707]. (*g*–*i*) Seeds typical of *Geleznowia* [*G. verrucosa*; *L. Broadhurst 14*, PERTH 5547822]. (*j*–*l*) Seeds typical of *P.* section *Erionema* [*P. verrucosa*; *MJB 249*, HO523410]. (*a*, *d*, *g*, *j*) Lateral views. (*b*, e, *h*, *k*) Adaxial views. (*c*, *f*, *i*, *l*) Longitudinal sections through the raphe. (*a*, *g*) Drawn with the placental portion of endocarp still attached to the seed; for all other drawings the placental endocarp was removed. Drawings are modified from Bayly (2001) and are not to scale.

smaller hilum that is round to deltoid and located, together with the raphe, on the adaxial face of the seed.

Our supermatrix approach expands on the results of previous molecular studies with more comprehensive sampling from *Philotheca* section *Philotheca*. Our results show *Philotheca* section *Philotheca* as polyphyletic, with members of this section falling into two separate clades, one including *Drummondita* and one sister to *Geleznowia* (Fig. 4).

The species of section *Philotheca* that group with *Drummondita* constitute (with the exception of *P. coateana*) an assemblage that, prior to the revision of Wilson (1998*a*), was considered the entirety of *Philotheca*. This narrow concept of *Philotheca* (referred to hereafter as *Philotheca* s.str.; Fig. 4, black triangle), first circumscribed by Bentham (1863), included only species with 10 fertile, monadelphous stamens and a spreading corolla. *Drummondita* also has monadelphous stamens, and this feature presumably led Mueller (1869) to include that genus in *Philotheca*. However, *Drummondita* was reinstated at generic rank by Wilson (1971) on the basis of key differences including stamen fertility (only five fertile in *Drummondita*), anther attachment (dorsifixed in *Drummondita*, versatile in *Philotheca*), petal texture

(glumaceous in *Drummondita*, soft in *Philotheca*) and carpel apex (unbeaked in *Drummondita* and beaked in *Philotheca*); as a result, *Philotheca* (*sensu* Wilson 1971) returned to its original, narrow circumscription. Wilson (1998*a*) expanded *Philotheca* to include *Philotheca* s.str., plus all species previously included by Wilson (1970) in *Eriostemon* section *Nigrostipulae*.

Among members of *Philotheca* s.str., fusion of the staminal filaments is present in *Philotheca salsolifolia*, *P. ciliata*, *P. basistyla*, *P. tubiflora*, *P. acrolopha* and *P. sericea* (Bayly 2001), but the degree of fusion varies among these species. In particular, the filaments of *P. acrolopha* and *P. sericea* are fused only very minutely at the base (Bayly 2001). In our analyses, the only species to be placed in this clade that does not have fused filaments is *Philotheca coateana*, which was not considered part of *Philotheca* s.str. by Bayly (2001); the free nature of filaments in this species was verified in the current study by using scanning electron microscopy (see Supplementary Fig. S5).

The remaining members of *Philotheca* section *Philotheca* that are not part of *Philotheca* s.str. are equivalent to *Eriostemon* section *Nigrostipulae sensu* Wilson (1970) (referred to herein as *Philotheca 'Nigrostipulae'*; Fig. 4, black square). In his revision of *Eriostemon*, Wilson (1998*a*) recognised the similarity of *Geleznowia* to his newly circumscribed *Philotheca* section *Philotheca* and contemplated that the arrangement he presented may render *Philotheca* paraphyletic with regards to *Geleznowia*. In particular, Wilson (1998*a*, 2013*a*) noted that *Geleznowia* and some members of *Philotheca* section *Philotheca* (including *Philotheca* s.str. and *Philotheca 'Nigrostipulae'*) possess filiform sclereids, similar seeds and the same chromosome number. Although *Geleznowia* shares these morphological features with *Philotheca* section *Philotheca* in the broad sense (*sensu* Wilson 1998*a*), our recovery of a sister relationship specifically between *Geleznowia* and *Philotheca 'Nigrostipulae'* is not supported by any morphological synapomorphies that we can identify, probably because of the highly derived morphology of *Geleznowia* and a high degree of morphological homoplasy in Clade 1.

Interpreting the backbone polytomy in the *Eriostemon* group

Is evolution multifurcating or are our data limited?

The amount of sequence data employed in our analyses represents a ~14-fold increase in dataset size compared with the most recent other studies on the group (106 885 bp in our phylogenomic alignment *v*. 7579 bp in Appelhans *et al.* 2021 and 5145 bp in Duretto *et al.* 2023). Even with this large dataset, we were unable to resolve backbone relationships between four supported major lineages of genera (Fig. 3). Across all analyses, these lineages were arranged on very short, unsupported branches that we have treated as a polytomy. Short divergences in molecular phylogenies may be explained by both biological and experimental causes. Biologically, polytomies can be the result of true multifurcations (so-called *hard* polytomies) caused by rapid radiation and simultaneous divergence events. However, polytomies may arise as a result of reaching the limit of resolution in the estimated tree (so-called *soft* polytomies) caused by using an insufficient amount of sequence data or sequence variation, conflicting data, or inappropriate methods of analysis (Slowinski 2001; Whitfield and Lockhart 2007; Lin *et al.* 2011; Sayyari and Mirarab 2018).

In ptDNA, conflicting phylogenetic signal may be attributed to topological incongruence among gene trees, noise introduced by site saturation, or applying substitution models uniformly across genes with differing rates of evolution.

The first of these causes belongs to the species tree paradigm (Doyle 2021), in which systematists infer species trees from gene trees under the multispecies coalescent (MSC) model that assumes free recombination between unlinked genes (Edwards 2009). Because of this assumption, coalescence-based approaches have generally been applied to studies utilising unlinked nuclear genes. However, several studies have reported conflicting phylogenetic signals among plastid genes (e.g. Zeng *et al.* 2014; Foster *et al.* 2018; Gonçalves *et al.* 2019), and the topic of whether these methods are suitable for analysing plastid loci (which have historically been treated as linked; Doyle 1997) has been subject to recent debate (Gonçalves *et al.* 2020; Doyle 2021). Although our analysis of tree space identified three different gene-tree clusters, estimation of the cluster phylogenies produced congruent topologies that differed mainly in their levels of branch support; thus, we found no evidence for conflicting signals among gene trees. This may reflect a failure of Robinson-Fould distances to adequately identify meaningful phylogenetic similarity (see Smith 2022), or simply show that there is no strong conflict among gene trees in each cluster. Instead of differences in tree topology among clusters, the identification of three gene-tree clusters may be the result of differing levels of phylogenetic informativeness across gene trees, with Cluster 1 containing, on average, the most informative genes with generally better-resolved topologies than for Clusters 2 and 3. We attribute the generally lower branch-support values displayed by our ASTRAL phylogeny to the lower resolving power of individual genes *v*. concatenated genes (Doyle 2021), rather than conflicting gene-tree topologies (this is also supported by gene discordance factors for the tree in Fig. 3; mean gCF: 41.9, mean gDF1: 5.8, mean gDF2: 5.6 across all branches; see Data availability for file).

Second, we are able to dismiss noise caused by site saturation as a potential source of conflict on the basis of the persistence of the polytomy in the analyses of the likelihood mapping subsets (with noisy loci removed), the DNA alignment partitioned by codon position, and the translated CDS alignment (Supplementary Fig. S6). Similarly, if rate

variation among loci were a contributor of conflict, then our IQ-TREE analysis partitioned by locus would have produced a result different from that from the unpartitioned analysis. Hence, we consider it unlikely that conflicting phylogenetic signal is a significant cause of the short, unsupported branches of the polytomy.

Previous molecular phylogenies of Rutaceae have resolved deeper relationships than that of our polytomy with far less ptDNA sequence data and comparable sequence variation (e.g. Groppo *et al.* 2008, 2012; Bayly *et al.* 2013; Appelhans *et al.* 2021). Several studies have also shown that lower-level relationships can be resolved using less data (e.g. Barrett *et al.* 2014; Bayly *et al.* 2016; Duretto *et al.* 2020, 2023). On the basis of these precedents, our dataset should be appropriate for resolving relationships at the taxonomic level of the polytomy. However, some biological characteristics of the plastome may render it inappropriate for resolving divergences that occurred over a short period of time. In plants, the plastome evolves at a relatively slow rate, at least half that of the nuclear genome (Wolfe *et al.* 1987). Genomes that evolve at slower rates are less capable of accumulating phylogenetically informative evolutionary changes during rapid radiations. In addition, lineage sorting is expected to progress more rapidly in ptDNA than in nDNA because of the smaller effective population size of the plastome (generally ¼ that of nuclear genes, with the exception of regions such as nuclear ribosomal DNA that are subjected to concerted evolution; Buckler and Holtsford 1996; Palumbi *et al.* 2001). Because of these features, the plastome may not be as useful as the nuclear genome for investigating lineages that have rapidly radiated, because there is less time for phylogenetically informative mutations to accumulate before lineages are sorted. If rapid radiation has occurred in the distant past, as is potentially the case in the *Eriostemon* group, this problem is likely to be compounded by subsequent lineage-specific mutations that can mask phylogenetically informative changes accumulated during the radiation (Whitfield and Lockhart 2007).

Our ASTRAL polytomy test was unable to reject that the polytomy is not a true multifurcation ($P > 0.5$ for all polytomy branches). However, as this test relies on calculating gene-tree topology likelihoods under the MSC model, the application of the test to our dataset of plastome loci is probably inappropriate (owing to divergence from the MSC model), and hence this result should be interpreted cautiously (Sayyari and Mirarab 2018; Doyle 2021).

Results from our tree-topology tests are likely to be more reliable. These showed a trend of higher support for topologies with Clade 1 as sister to the rest of the *Eriostemon* group, and low support for a multifurcating topology, suggesting that relationships between these lineages are perhaps more likely to be bifurcating rather than multifurcating.

The true nature of relationships around the backbone polytomy in the *Eriostemon* group remains difficult to answer with the current dataset, and we suggest that further investigation using more appropriate data, in particular, multi-locus nuclear DNA markers, is required before any conclusions are made regarding the *hard* or *soft* status of the polytomy. Clarification of the polytomy, and its *hard* or *soft* status, will also allow for interpretation of the higher-level branching order and evolution of the group.

The significance of understanding the polytomy

Together, the clades that make up the backbone polytomy in the *Eriostemon* group (i.e. Clades 1–4) contain 16 genera (13 Australian) and ~204 species (~194 Australian) that include a large proportion of Australia's Rutaceae diversity (total ~42 genera, ~490 spp.). Taxa in the *Eriostemon* group account for nearly all of the Rutaceae that occur on low-nutrient soils in dry sclerophyll communities in the south-east and south-west of Australia (Hartley 1995); the only genera outside this group that occur in similar habitat are *Boronia* (~125 spp. in Australia), *Zieria* (~63 spp. in eastern Australia), *Neobyrnesia* (1 sp. in N Northern Territory) and *Cyanothamnus* (23 spp. in Australia). Because of this, they are an important component of the Australian flora.

The phylogenetic depth at which the polytomy occurs means that it is largely irrelevant to the taxonomic delimitation of genera but may be pertinent to higher-level classification. Currently, revisions of tribal and subtribal classification are needed for Rutaceae (Appelhans *et al.* 2021). A new tribal classification would probably apply above the level of the polytomy and, hence, not require its resolution, but a robust future subtribal classification would certainly benefit from the resolution of the branching order of Clades 1–4. Subtribes in the *Eriostemon* group have been largely neglected since Engler (1931), who placed the contemporary genera (*Muiriantha* was not yet described) in the *Eriostemon* group across the following four subtribes: Eriostemoninae (including *Asterolasia*, *Crowea*, *Drummondita* (as a section of *Philotheca*), *Eriostemon*, *Geleznowia*, *Leionema* (as a section of *Phebalium*), *Phebalium* and *Philotheca*), Nematolepidinae (*Chorilaena* and *Nematolepis*), Correinae (monotypic, including *Correa*) and Diplolaeninae (monotypic, including *Diplolaena*). Under this scheme, Eriostemoninae is polyphyletic. On the basis of our phylogeny, one could propose a new system that recognises each of the major lineages of the group (i.e. Clades 1–4) as separate subtribes. Alternatively, subtribe Eriostemoninae could be split into several different subtribes so as to retain Correinae, Diplolaeninae and Nematolepidinae. In any case, a newly proposed classification should be constructed with consideration of relationships across the whole of the Rutaceae to ensure that taxonomic ranks are applied in a consistent manner, and should also consider the morphological diagnosability of subtribes, something that the current study does not thoroughly do.

Beyond taxonomic classification, resolving the branching order of the polytomy would prove useful to studies focussed on macroevolution and biogeography. In terms of morphology, the *Eriostemon* group displays multiple

characters of biological and ecological interest that have evidently experienced state transitions (e.g. in floral features and phyllotaxy); studies investigating the evolutionary histories of characters by using methods that require bifurcating phylogenetic frameworks, such as ancestral-state reconstructions, would be enabled by resolution of the polytomy. Biogeographically, the *Eriostemon* group is noteworthy for having multiple genera that are disjunct between south-western and south-eastern Australia (e.g. *Phebalium*, 16 spp. in south-west, 22 spp. in south-east; *Nematolepis*, 1 sp. in south-west, 6 spp. in south-east; *Philotheca* section *Erionema*, 1 sp. in south-west, 14 spp. in south-east; *Asterolasia*, 5 spp. in south-west, 14 spp. in south-east). This distribution pattern occurs in many plant taxa and has been attributed to vicariance associated with marine inundations of south-central Australia and subsequent edaphic and climatic barriers during the mid-Miocene (~16–14 million years ago; Crisp and Cook 2007; Ladiges *et al.* 2010, 2012). Compared with other species-rich families in Australia, the Rutaceae is unconventional in having a higher net diversification rate of genera in the south-east than in the south-west from the Eocene–Oligocene (~34 million years ago) extinction pulse until the mid-Miocene (Nge *et al.* 2020). Resolution of the backbone polytomy would enable the further testing of hypotheses relating to the timing of this vicariance event in the Australian Rutaceae and offer insight into the drivers of generic diversification, and, specifically, whether the diversification of major lineages (i.e. our Clades 1–4) was influenced by such an event. It could also present an opportunity to provide a more robust timing for the split of *Myrtopsis* in New Caledonia.

Future classification of *Philotheca*

The recovery of *Philotheca* as polyphyletic in our analyses is consistent with previous work (Bayly *et al.* 2013; Appelhans *et al.* 2021; Duretto *et al.* 2023), and here we have provided further clarification of this taxonomic issue. Prior to the current study, the best estimate of relationships in *Philotheca* was provided by Duretto *et al.* (2023). Our analyses and that of Duretto *et al.* (2023) both suggest that *Philotheca* section *Corynonema* and *Philotheca* section *Cyanochlamys* are phylogenetically distant from the type of the genus (*P. salsolifolia*). Undoubtedly, they should be placed in separate genera from *Philotheca* and each other. However, in the case of *P.* section *Cyanochlamys*, contrasting support for monophyly (ptDNA; Fig. 3) *v.* paraphyly (nrDNA; see the Supplementary 'Methods and results' section) in our analyses raises questions about the appropriate taxonomic status of that group relative to the related, monotypic genus *Muiriantha*.

Within Clade 1, we have identified three ptDNA lineages of *Philotheca* species that render *Philotheca* paraphyletic with respect to *Drummondita* and *Geleznowia*, namely the following: (1) *Philotheca* section *Erionema*, supported as monophyletic and sister to the rest of the clade; (2) *Philotheca* s.str., not resolved as monophyletic but strongly placed in a clade with *Drummondita*; and (3) *Philotheca 'Nigrostipulae'*, supported as monophyletic and sister to *Geleznowia*. Taxonomic interpretation of these relationships could include 'lumping' (e.g. placing all of Clade 1 in a single genus, *Philotheca*) or 'splitting' to various extents. Given that many of the species in this clade have been sampled only for a small number of plastid markers (Fig. 4), and that nrDNA sampling here (see the Supplementary 'Methods and results' section) and by Duretto *et al.* (2023) is very limited and does not resolve distinct nrDNA groups corresponding to *Philotheca* s.str. and *Philotheca* '*Nigrostipulae*', some aspects of relationships in the group remain uncertain.

Given limitations of the results presented here, and the new questions they have raised, we consider that further investigation of the relationships of *Philotheca* is warranted before taxonomic changes are proposed. In particular, sequencing approaches that generate large amounts of data from the nuclear genome, such as using the MyBaits Expert Plant Angiosperms353 bait set (Arbor Bioscience, Ann Arbor, MI, USA; Johnson *et al.* 2019) for target-sequence capture (H. K. Orel, unpubl. data), could prove useful for elucidating unresolved relationships, because of the faster evolutionary rates of nuclear genes. Such data would also enable comparison with the ptDNA results presented here so as to evaluate the extent of cytonuclear discordance in this group.

Conclusions

This study has identified four major lineages of genera in the *Eriostemon* group with high support, significantly improving understanding of generic relationships in the Australasian Rutaceae (subfam. Zanthoxyloideae). Our analyses of full plastome sequences were unable to resolve the branching order of these major lineages; thus, they were treated as a polytomy and the true phylogenetic arrangement of the lineages remains unclear. Tests to clarify and identify the cause of this polytomy were inconclusive, but suggested greater support for topologies with the *Philotheca–Drummondita–Geleznowia* alliance (Clade 1) sister to the three other major lineages. This result also indicated that a bifurcating resolution of the polytomy is probably possible with a dataset more appropriate for investigating this question. Although the methods that we used to investigate the polytomy ultimately did not result in its resolution, we feel that these approaches are likely to be more powerful when applied to nDNA sequence data, because they are largely aimed at detecting and dealing with discordant phylogenetic signal across independently evolving loci or genes. Consequently, future phylogenomic studies of the *Eriostemon* group using sequence data from the nuclear genome hold much promise for improving phylogenetic resolution of the polytomy. Finally, our results reinforced previous

findings that *Philotheca* is polyphyletic, and raised new questions regarding current sectional limits and monophyly that require further investigation before taxonomic changes can be made.

Note added in proof

In the period of time between acceptance and publication of this paper, a study on *Geleznowia* has been published that has increased the number of species in *Geleznowia* from two to seven (Anderson *et al*. 2023).

Supplementary material

Supplementary material is available online.

References

Anderson BM, Binks RM, Byrne M, Crawford AD, Shepherd KA (2023) Using RADseq to resolve species boundaries in a morphologically complex group of yellow-flowered shrubs (Geleznowia, Rutaceae). *Australian Systematic Botany* **36**(4), 277–311. doi:10.1071/SB23010

Appelhans MS, Bayly MJ, Heslewood MM, Groppo M, Verboom GA, Forster PI, Kallunki JA, Duretto MF (2021) A new subfamily classification of the *Citrus* family (Rutaceae) based on six nuclear and plastid markers. *Taxon* **70**, 1035–1061. doi:10.1002/tax.12543

Armstrong JA (1979) Biotic pollination mechanisms in the Australian flora – a review. *New Zealand Journal of Botany* **17**, 467–508. doi:10.1080/0028825X.1979.10432565

Armstrong JA (1987) Pollination syndromes as generic determinants. *Australian Systematic Botany Society Newsletter* **53**, 54–59.

Armstrong JA (1991) Studies on pollination and systematics in the Australian Rutaceae. PhD thesis, University of New South Wales, Sydney, NSW, Australia. Available at http://hdl.handle.net/1959.4/59714

Baker WJ, Bailey P, Barber V, Barker A, Bellot S, Bishop D, Botigué LR, Brewer G, Carruthers T, Clarkson JJ, Cook J (2022) A comprehensive phylogenomic platform for exploring the angiosperm tree of life. *Systematic Biology* **71**, 301–319. doi:10.1093/sysbio/syab035

Bardon L, Sothers C, Prance GT, Malé P-JG, Xi Z, Davis CC, Murienne J, García-Villacorta R, Coissac E, Lavergne S, Chave J (2016) Unraveling the biogeographical history of Chrysobalanaceae from plastid genomes. *American Journal of Botany* **103**, 1089–1102. doi:10.3732/ajb.1500463

Barrett RA, Bayly MJ, Duretto MF, Forster PI, Ladiges PY, Cantrill DJ (2014) A chloroplast phylogeny of *Zieria* (Rutaceae) in Australia and New Caledonia shows widespread incongruence with species-level taxonomy. *Australian Systematic Botany* **27**, 427–449. doi:10.1071/SB14033

Batty EL, Holmes GD, Murphy DJ, Forster PI, Neal WC, Bayly MJ (2022) Phylogeny, classification and biogeography of *Philotheca* sect. *Erionema* (Rutaceae) based on nrDNA sequences. *Australian Systematic Botany* **35**, 326–338. doi:10.1071/SB22003

Bayly MJ (2001) A cladistic and biogeographic analysis of *Philotheca* (Rutaceae) and allied genera. PhD thesis, The University of Melbourne, Melbourne, Vic., Australia. Available at http://hdl.handle.net/11343/37369

Bayly MJ, Holmes GD, Forster PI, Cantrill DJ, Ladiges PY (2013) Major clades of Australasian Rutoideae (Rutaceae) based on *rbcL* and *atpB* sequences. *PLoS One* **8**, e72493. doi:10.1371/journal.pone.0072493

Bayly MJ, Holmes GD, Forster PI, Munzinger J, Cantrill DJ, Ladiges PY (2016) Phylogeny, classification and biogeography of *Halfordia* (Rutaceae) in Australia and New Caledonia. *Plant Systematics and Evolution* **302**, 1457–1470. doi:10.1007/s00606-016-1344-0

Bentham G (1863) 'Flora australiensis. Vol. 1.' (Lovell Reeve: London, UK)

Broadhurst LM, Tan BH (2001) Floral biology of the Western Australian endemic 'yellow bells', Geleznowia verrucosa Turcz (Rutaceae). *Journal of the Royal Society of Western Australia* **84**, 83–89.

Bryant D, Moulton V (2002) NeighborNet: an agglomerative method for the construction of planar phylogenetic networks. In 'Algorithms in Bioinformatics, WABI 2002, LNCS 2452'. (Eds R Guigó, D Gusfield) pp. 375–391. (Springer-Verlag)

Buckler ES, Holtsford TP (1996) *Zea* systematics: ribosomal *ITS* evidence. *Molecular Biology and Evolution* **13**, 612–622. doi:10.1093/oxfordjournals.molbev.a025621

Clowes C, Fowler RM, Fahey PS, Kellermann J, Brown GK, Bayly MJ (2022) Big trees of small baskets: phylogeny of the Australian genus *Spyridium* (Rhamnaceae: Pomaderreae), focusing on biogeographic patterns and species circumscriptions. *Australian Systematic Botany* **35**, 95–119. doi:10.1071/SB21034

Crisp MD, Cook LG (2007) A congruent molecular signature of vicariance across multiple plant lineages. *Molecular Phylogenetics and Evolution* **43**, 1106–1117. doi:10.1016/j.ympev.2007.02.030

da Silva MFGF, Gottlieb OR, Ehrendorfer F (1988) Chemosystematics of the Rutaceae: suggestions for a more natural taxonomy and evolutionary interpretation of the family. *Plant Systematics and Evolution* **161**, 97–134. doi:10.1007/BF00937293

Doyle JJ (1997) Trees within trees: genes and species, molecules and morphology. *Systematic Biology* **46**, 537–553. doi:10.1093/sysbio/46.3.537

Doyle JJ (2021) Defining coalescent genes: theory meets practice in organelle phylogenomics. *Systematic Biology* **71**, 476–489. doi:10.1093/sysbio/syab053

Duchêne DA, Bragg JG, Duchêne S, Neaves LE, Potter S, Moritz C, Johnson RN, Ho SYW, Eldridge MDB (2018) Analysis of phylogenomic tree space resolves relationships among marsupial families. *Systematic Biology* **67**, 400–412. doi:10.1093/sysbio/syx076

Duretto MF, Heslewood MM, Bayly MJ (2020) *Boronia* (Rutaceae) is polyphyletic: reinstating *Cyanothamnus* and the problems associated with inappropriately defined outgroups. *Taxon* **69**, 481–499. doi:10.1002/tax.12242

Duretto MF, Heslewood MM, Bayly MJ (2023) Generic and infrageneric limits of *Phebalium* and its allies (Rutaceae: Zanthoxyloideae). *Australian Systematic Botany* **36**, 107–142. doi:10.1071/SB22018

Edwards SV (2009) Is a new and general theory of molecular systematics emerging. *Evolution* **63**, 1–19. doi:10.1111/j.1558-5646.2008.00549.x

Engler A (1874) Rutaceae. In 'Flora Brasiliensis. Vol. 12 (2)'. (Eds CFP Martius, AW Eichler) pp. 79–195. (Frid. Fleischer: Leipzig, German Empire)

Engler A (1896) Rutaceae. In 'Die Natürlichen Pflanzenfamilien. Vol. III'. pp. 95–201. (Wilhelm Engelmann: Leipzig, German Empire)

Engler A (1931) Rutaceae. In 'Die Natürlichen Pflanzenfamilien, 2nd edn. Vol. 19a'. (Eds A Engler, K Prantl) pp. 187–359. (Wilhelm Engelmann: Leipzig, German Republic)

Foster CSP, Henwood MJ, Ho SYW (2018) Plastome sequences and exploration of tree-space help to resolve the phylogeny of riceflowers (Thymelaeaceae: *Pimelea*). *Molecular Phylogenetics and Evolution* **127**, 156–167. doi:10.1016/j.ympev.2018.05.018

French PA, Brown GK, Bayly MJ (2016) Incongruent patterns of nuclear and chloroplast variation in *Correa* (Rutaceae): introgression and biogeography in south-eastern Australia. *Plant Systematics and Evolution* **302**, 447–468. doi:10.1007/s00606-016-1277-7

Gonçalves DJP, Simpson BB, Ortiz EM, Shimizu GH, Jansen RK (2019) Incongruence between gene trees and species trees and phylogenetic signal variation in plastid genes. *Molecular Phylogenetics and Evolution* **138**, 219–232. doi:10.1016/j.ympev.2019.05.022

Gonçalves DJP, Jansen RK, Ruhlman TA, Mandel JR (2020) Under the rug: abandoning persistent misconceptions that obfuscate organelle evolution. *Molecular Phylogenetics and Evolution* **151**, 106903. doi:10.1016/j.ympev.2020.106903

Grandcolas P (2017) Ten false ideas about New Caledonia biogeography. *Cladistics* **33**, 481–487. doi:10.1111/cla.12176

Groppo M, Pirani JR, Salatino MLF, Blanco SR, Kallunki JA (2008) Phylogeny of Rutaceae based on two noncoding regions from cpDNA. *American Journal of Botany* **95**, 985–1005. doi:10.3732/ajb.2007313

Groppo M, Kallunki JA, Pirani JR, Antonelli A (2012) Chilean *Pitavia* more closely related to Oceania and Old World Rutaceae than to

Neotropical groups: evidence from two cpDNA non-coding regions, with a new subfamilial classification of the family. *PhytoKeys* **19**, 9–29. doi:10.3897/phytokeys.19.3912

Guindon S, Dufayard J-F, Lefort V, Anisimova M, Hordijk W, Gascuel O (2010) New algorithms and methods to estimate maximum-likelihood phylogenies: assessing the performance of PhyML 3.0. *Systematic Biology* **59**, 307–321. doi:10.1093/sysbio/syq010

Hammer TA, Zhong X, Colas des Francs-Small C, Nevill PG, Small ID, Thiele KR (2019) Resolving intergeneric relationships in the aervoid clade and the backbone of *Ptilotus* (Amaranthaceae): evidence from whole plastid genomes and morphology. *Taxon* **68**, 297–314. doi:10.1002/tax.12054

Hartley TG (1995) A new combination in *Boronella* (Rutaceae) and a view on relationships of the genus. *Adansonia* **17**, 107–111.

Hartley TG (2001) Morphology and biogeography in Australasian–Malesian Rutaceae. *Malayan Nature Journal* **55**, 197–220.

Hartley TG (2003) *Neoschmidia*, a new genus of Rutaceae from New Caledonia. *Adansonia* **25**, 7–12.

Hoang DT, Chernomor O, von Haeseler A, Minh BQ, Vinh LS (2018) UFBoot2: improving the ultrafast bootstrap approximation. *Molecular Biology and Evolution* **35**, 518–522. doi:10.1093/molbev/msx281

Hou N, Wang G, Feng SJ, Wei AZ (2018) The complete chloroplast genome of an aromatic Chinese pepper (*Zanthoxylum simulans*). *Mitochondrial DNA Part B* **3**, 26–27. doi:10.1080/23802359.2017.1419082

Huson DH, Bryant D (2006) Application of phylogenetic networks in evolutionary studies. *Molecular Biology and Evolution* **23**, 254–267. doi:10.1093/molbev/msj030

Jin J-J, Yu W-B, Yang J-B, Song Y, DePamphilis CW, Yi T-S, Li D-Z (2020) GetOrganelle: a fast and versatile toolkit for accurate de novo assembly of organelle genomes. *Genome Biology* **21**, 241. doi:10.1186/s13059-020-02154-5

Johnson MG, Pokorny L, Dodsworth S, Botigué LR, Cowan RS, Devault A, Eiserhardt WL, Epitawalage N, Forest F, Kim JT, Leebens-Mack JH, Leitch IJ, Maurin O, Soltis DE, Soltis PS, Wong GK, Baker WJ, Wickett NJ (2019) A universal probe set for targeted sequencing of 353 nuclear genes from any flowering plant designed using k-medoids clustering. *Systematic Biology* **68**, 594–606. doi:10.1093/sysbio/syy086

Jombart T, Kendall M, Almagro-Garcia J, Colijn C (2017) treespace: statistical exploration of landscapes of phylogenetic trees. *Molecular Ecology Resources* **17**, 1385–1392. doi:10.1111/1755-0998.12676

Joyce EM, Appelhans MS, Buerki S, *et al.* (2023) Phylogenomic analyses of Sapindales support new family relationships, rapid Mid-Cretaceous Hothouse diversification, and heterogeneous histories of gene duplication. *Frontiers in Plant Science* **14**, 1063174. doi:10.3389/fpls.2023.1063174

Kalyaanamoorthy S, Minh BQ, Wong TKF, von Haeseler A, Jermiin LS (2017) ModelFinder: fast model selection for accurate phylogenetic estimates. *Nature Methods* **14**, 587–589. doi:10.1038/nmeth.4285

Katoh K, Standley DM (2013) MAFFT multiple sequence alignment software version 7: improvements in performance and usability. *Molecular Biology and Evolution* **30**, 772–780. doi:10.1093/molbev/mst010

Katoh K, Misawa K, Kuma K-i, Miyata T (2002) MAFFT: a novel method for rapid multiple sequence alignment based on fast Fourier transform. *Nucleic Acids Research* **30**, 3059–3066. doi:10.1093/nar/gkf436

Kishino H, Hasegawa M (1989) Evaluation of the maximum likelihood estimate of the evolutionary tree topologies from DNA sequence data, and the branching order in hominoidea. *Journal of Molecular Evolution* **29**, 170–179. doi:10.1007/bf02100115

Kishino H, Miyata T, Hasegawa M (1990) Maximum likelihood inference of protein phylogeny and the origin of chloroplasts. *Journal of Molecular Evolution* **31**, 151–160. doi:10.1007/BF02109483

Kubitzki K, Kallunki JA, Duretto M, Wilson PG (2011) Rutaceae. In 'Flowering Plants. Eudicots: Sapindales, Cucurbitales, Myrtaceae'. (Ed. K Kubitzki) pp. 276–356. (Springer)

Ladiges PY, Cantrill D (2007) New Caledonia-Australian connections: biogeographic patterns and geology. *Australian Systematic Botany* **20**, 383–389. doi:10.1071/SB07018

Ladiges PY, Bayly MJ, Nelson GJ (2010) East–west continental vicariance in *Eucalyptus* subgenus *Eucalyptus*. In 'Beyond Cladistics. The Branching of a Paradigm'. (Eds DM Williams, S Knapp) pp. 267–302. (University of California Press: Berkeley, CA, USA)

Ladiges PY, Bayly MJ, Nelson G (2012) Searching for ancestral areas and artifactual centers of origin in biogeography: with comment on east–west patterns across southern Australia. *Systematic Biology* **61**, 703–708. doi:10.1093/sysbio/sys005

Lin GN, Zhang C, Xu D (2011) Polytomy identification in microbial phylogenetic reconstruction. *BMC Systems Biology* **5**, S2. doi:10.1186/1752-0509-5-S3-S2

Minh BQ, Hahn MW, Lanfear R (2020*a*) New methods to calculate concordance factors for phylogenomic datasets. *Molecular Biology and Evolution* **37**, 2727–2733. doi:10.1093/molbev/msaa106

Minh BQ, Schmidt HA, Chernomor O, Schrempf D, Woodhams MD, von Haeseler A, Lanfear R (2020*b*) IQ-TREE 2: new models and efficient methods for phylogenetic inference in the genomic era. *Molecular Biology and Evolution* **37**, 1530–1534. doi:10.1093/molbev/msaa015

Mole BJ, Udovicic F, Ladiges PY, Duretto MF (2004) Molecular phylogeny of *Phebalium* (Rutaceae: Boronieae) and related genera based on the nrDNA regions ITS 1 + 2. *Plant Systematics and Evolution* **249**, 197–212. doi:10.1007/s00606-004-0218-z

Mueller F (1869) 'Fragmenta phytographiæ Australiæ. Vol. 7.' (Auctoritate Guberni Coloniæ Victoriæ, Ex Officina Joannis Ferres: Melbourne, Australia) Available at https://www.biodiversitylibrary.org/item/7224

Nattier R, Pellens R, Robillard T, Jourdan H, Legendre F, Caesar M, Nel A, Grandcolas P (2017) Updating the phylogenetic dating of New Caledonian biodiversity with a meta-analysis of the available evidence. *Scientific Reports* **7**, 3705. doi:10.1038/s41598-017-02964-x

Neal WC, James EA, Bayly MJ (2019) Phylogeography, classification and conservation of pink zieria (*Zieria veronicea*; Rutaceae): influence of changes in climate, geology and sea level in south-eastern Australia. *Plant Systematics and Evolution* **305**, 503–520. doi:10.1007/s00606-019-01589-z

Nge FJ, Biffin E, Thiele KR, Waycott M (2020) Extinction pulse at Eocene–Oligocene boundary drives diversification dynamics of two Australian temperate floras. *Proceedings of the Royal Society of London – B. Biological Sciences* **287**, 20192546. doi:10.1098/rspb.2019.2546

Orchard AE (1999) Introduction. In 'Flora of Australia. Vol. 1 – Introduction'. (Ed. AE Orchard) pp. 1–9. (ABRS: Canberra, ACT, Australia; and CSIRO Australia: Melbourne, Vic., Australia)

Othman RNA, Jordan GJ, Worth JRP, Steane DA, Duretto MF (2010) Phylogeny and infrageneric classification of Correa Andrews (Rutaceae) on the basis of nuclear and chloroplast DNA. *Plant Systematics and Evolution* **288**, 127–138. doi:10.1007/s00606-010-0315-0

Palumbi SR, Cipriano F, Hare MP (2001) Predicting nuclear gene coalescence from mitochondrial data: the three-times rule. *Evolution* **55**, 859–868. doi:10.1554/0014-3820(2001)055[0859:PNGCFM]2.0.CO;2

Penny D, Hendy MD (1985) The use of tree comparison metrics. *Systematic Zoology* **34**, 75–82. doi:10.2307/2413347

Rambaut A, Drummond AJ, Xie D, Baele G, Suchard MA (2018) Posterior summarization in Bayesian phylogenetics using Tracer 1.7. *Systematic Biology* **67**, 901–904. doi:10.1093/sysbio/syy032

Revell LJ (2012) phytools: an R package for phylogenetic comparative biology (and other things). *Methods in Ecology and Evolution* **3**, 217–223. doi:10.1111/j.2041-210X.2011.00169.x

Rieseberg LH, Soltis DE (1991) Phylogenetic consequences of cytoplasmic gene flow in plants. *Evolutionary Trends in Plants* **5**, 65–84.

Ronquist F, Teslenko M, van der Mark P, Ayres DL, Darling A, Höhna S, Larget B, Liu L, Suchard MA, Huelsenbeck JP (2012) MrBayes 3.2: efficient Bayesian phylogenetic inference and model choice across a large model space. *Systematic Biology* **61**, 539–542. doi:10.1093/sysbio/sys029

Sang T, Crawford DJ, Stuessy TF (1997) Chloroplast DNA phylogeny, reticulate evolution, and biogeography of *Paeonia* (Paeoniaceae). *American Journal of Botany* **84**, 1120–1136. doi:10.2307/2446155

Sayyari E, Mirarab S (2018) Testing for polytomies in phylogenetic species trees using quartet frequencies. *Genes* **9**, 132. doi:10.3390/genes9030132

Schuster TM, Setaro SD, Tibbits JFG, Batty EL, Fowler RM, McLay TGB, Wilcox S, Ades PK, Bayly MJ (2018) Chloroplast variation is incongruent with classification of the Australian bloodwood eucalypts (genus Corymbia, family Myrtaceae). *PLoS One* **13**, e0195034. doi:10.1371/journal.pone.0195034

Shepherd LD, McLay TGB (2011) Two micro-scale protocols for the isolation of DNA from polysaccharide-rich plant tissue. *Journal of Plant Research* **124**, 311–314. doi:10.1007/s10265-010-0379-5

Shimodaira H (2002) An approximately unbiased test of phylogenetic tree selection. *Systematic Biology* **51**, 492–508. doi:10.1080/10635150290069913

Shimodaira H, Hasegawa M (1999) Multiple comparisons of log-likelihoods with applications to phylogenetic inference. *Molecular Biology and Evolution* **16**, 1114–1116. doi:10.1093/oxfordjournals.molbev.a026201

Slowinski JB (2001) Molecular Polytomies. *Molecular Phylogenetics and Evolution* **19**, 114–120. doi:10.1006/mpev.2000.0897

Smith MR (2022) Robust Analysis of Phylogenetic Tree Space. *Systematic Biology* **71**, 1255–1270. doi:10.1093/sysbio/syab100

Smith-White S (1954) Chromosome numbers in the Boronieae (Rutaceae) and their bearing on the evolutionary development of the tribe in the Australian flora. *Australian Journal of Botany* **2**, 287–303. doi:10.1071/BT9540287

Stace HM, Armstrong JA (1992) New chromosome numbers for Rutaceae. *Australian Systematic Botany* **5**, 501–505. doi:10.1071/SB9920501

Stamatakis A (2014) RAxML version 8: a tool for phylogenetic analysis and post-analysis of large phylogenies. *Bioinformatics* **30**, 1312–1313. doi:10.1093/bioinformatics/btu033

Strimmer K, Rambaut A (2002) Inferring confidence sets of possibly misspecified gene trees. *Proceedings of the Royal Society of London – B. Biological Sciences* **269**, 137–142. doi:10.1098/rspb.2001.1862

Strimmer K, von Haeseler A (1997) Likelihood-mapping: a simple method to visualize phylogenetic content of a sequence alignment. *Proceedings of the National Academy of Sciences* **94**, 6815–6819. doi:10.1073/pnas.94.13.6815

Tate JA, Simpson BB (2003) Paraphyly of *Tarasa* (Malvaceae) and diverse origins of the polyploid species. *Systematic Botany* **28**, 723–737. doi:10.1043/02-64.1

Telford IRH, Bruhl JJ (2020) Morphological data indicate the subspecies of *Leionema elatius* (Rutaceae) are not conspecific. *Telopea* **23**, 197–203. doi:10.7751/telopea14433

Tibshirani R, Walther G, Hastie T (2001) Estimating the number of clusters in a data set via the gap statistic. *Journal of the Royal Statistical Society: Series B (Statistical Methodology)* **63**, 411–423. doi:10.1111/1467-9868.00293

Tillich M, Lehwark P, Pellizzer T, Ulbricht-Jones ES, Fischer A, Bock R, Greiner S (2017) GeSeq – versatile and accurate annotation of organelle genomes. *Nucleic Acids Research* **45**, W6–W11. doi:10.1093/nar/gkx391

Toews DPL, Brelsford A (2012) The biogeography of mitochondrial and nuclear discordance in animals. *Molecular Ecology* **21**, 3907–3930. doi:10.1111/j.1365-294X.2012.05664.x

Tsitrone A, Kirkpatrick M, Levin DA (2003) A model for chloroplast capture. *Evolution* **57**, 1776–1782. doi:10.1111/j.0014-3820.2003.tb00585.x

Whitfield JB, Lockhart PJ (2007) Deciphering ancient rapid radiations. *Trends in Ecology & Evolution* **22**, 258–265. doi:10.1016/j.tree.2007.01.012

Williams AV, Miller JT, Small I, Nevill PG, Boykin LM (2016) Integration of complete chloroplast genome sequences with small amplicon datasets improves phylogenetic resolution in *Acacia*. *Molecular Phylogenetics and Evolution* **96**, 1–8. doi:10.1016/j.ympev.2015.11.021

Wilson PG (1970) A taxonomic revision of the genera *Crowea*, *Eriostemon* and *Phebalium* (Rutaceae). *Nuytsia* **1**, 3–155. doi:10.58828/nuy00001

Wilson PG (1971) Taxonomic notes on the family Rutaceae, principally of Western Australia. *Nuytsia* **1**, 197–207. doi:10.58828/nuy00004

Wilson PG (1998*a*) A taxonomic review of the genera *Eriostemon* and *Philotheca* (Rutaceae: Boronieae). *Nuytsia* **12**, 239–265.

Wilson PG (1998*b*) New species and nomenclatural changes in *Phebalium* and related genera (Rutaceae). *Nuytsia* **12**, 267–288.

Wilson PG (2013*a*) Philotheca. In 'Flora of Australia. Vol. 26, Meliaceae, Rutaceae, Zygophyllaceae'. (Ed. A Wilson) pp. 336–415. (ABRS: Canberra, ACT, Australia; and CSIRO Australia: Melbourne, Vic., Australia)

Wilson PG (2013*b*) Muiriantha. In 'Flora of Australia. Vol. 26, Meliaceae, Rutaceae, Zygophyllaceae'. (Ed. A Wilson) p. 447. (ABRS: Canberra, ACT, Australia; and CSIRO Australia: Melbourne, Vic., Australia)

Wolfe KH, Li WH, Sharp PM (1987) Rates of nucleotide substitution vary greatly among plant mitochondrial, chloroplast, and nuclear DNAs. *Proceedings of the National Academy of Sciences* **84**, 9054–9058. doi:10.1073/pnas.84.24.9054

Zeng L, Zhang Q, Sun R, Kong H, Zhang N, Ma H (2014) Resolution of deep angiosperm phylogeny using conserved nuclear genes and estimates of early divergence times. *Nature Communications* **5**, 4956. doi:10.1038/ncomms5956

Zhang C, Rabiee M, Sayyari E, Mirarab S (2018) ASTRAL-III: polynomial time species tree reconstruction from partially resolved gene trees. *BMC Bioinformatics* **19**, 153. doi:10.1186/s12859-018-2129-y

Data availability. GenBank accession numbers for the sequences used in this study can be found in Table 1. The datasets generated and analysed during the current study are available in the Figshare repository (https://doi.org/10.26188/21761735). N.B.: as several taxonomic revisions were made during this study, sequences in the Figshare datasets may not incorporate the taxonomic changes of Duretto *et al.* (2020, 2023) and Telford and Bruhl (2020), which are incorporated in this paper. Specifically, sequences of *Leionema beckleri* (PIF33439), *Cyanothamnus anemonifolius* (MJB2562), *Chorilaena anceps* (BJM475), *Chorilaena euphemiae* (BJM424) and *Phebalium multiflorum* (RB1280) may be respectively named *Leionema elatius*, *Boronia anemonifolia*, *Rhadinothamnus anceps*, *Rhadinothamnus euphemiae* and *Microcybe multiflora*.

Conflicts of interest. M. J. Bayly is an editor for *Australian Systematic Botany*. Despite this relationship, he did not at any stage have editor-level access to this manuscript while in peer review, as is the standard practice when handling manuscripts submitted by an editor to this journal. *Australian Systematic Botany* encourages its editors to publish in the journal and has protocols that keep editors separate from the decision-making processes for their manuscripts. The authors have no conflicts of interests to declare that are relevant to the content of this article.

Declaration of funding. This research was supported by an Early Career Researcher Grant from The University of Melbourne. It also used collections made under previous grants from the Australian Research Council (grant LP0776737) and Australian Biological Resources Study (grant PD208-02). H. K. Orel is supported by an Australian Government Research Training Program scholarship, and a Sophie Ducker scholarship from the University of Melbourne Botany Foundation.

Acknowledgements. The authors thank Bryan Mole, Adrienne Markey, Jeremy Bruhl, Daniel Ohlsen, Mike Mathieson, Gillian Brown, Peter Wilson and Adele Gibbs for assistance with fieldwork or provision and use of samples; and Freya Berwick, Katie Roland, Miranda Boyle (all intern students), Jessie Knott, Erin Batty, Gareth Holmes, Rachael Fowler, and Stephen Wilcox for assistance with laboratory work or DNA sequencing. Collecting permits were provided by the former Victorian Department of Sustainability and Environment, NSW National Parks and Wildlife Service, South Australian Department of Environment and Heritage, the former Western Australian Department of Environment and Conservation, and the former Queensland Environmental Protection Agency.

Author contributions. M. J. Bayly and H. K. Orel conceived the ideas and experimental design for this study. P. I. Forster and M. J. Bayly contributed samples. W. C. Neal, T. G. B. McLay and M. J. Bayly performed laboratory work to generate the sequence data. H. K. Orel assembled the sequence data and conducted all analyses; T. G. B. McLay assisted with topology testing and preliminary analyses. Results were interpreted by H. K. Orel, T. G. B. McLay and M. J. Bayly. H. K. Orel led the writing, with input from all other authors.

Author affiliations

[A]School of Biosciences, The University of Melbourne, Parkville, Vic. 3010, Australia.

[B]Royal Botanic Gardens Victoria, Melbourne, Vic. 3004, Australia.

[C]Queensland Herbarium & Biodiversity Science, Department of Environment & Science, Brisbane Botanic Gardens, Toowong, Qld 4066, Australia.